Report on the intercomparison of reference materials used to measure luminance and reduced luminance coefficients of road surfaces in the laboratory and on-site software for *q* measurement uncertainty evaluation

EMPIR GRANT Agreement 16NRM02 SURFACE

Draft 0.3

Paola Iacomussi- INRIM, Istituto Nazionale di Ricerca Metrologica, Torino, Italy
Dominique Renoux – LNE , Laboratoire Nationale des Essais, Paris, France
Valérie Muzet – Cerema, Research team ENDSUM, Strasbourg, France
Mikael Lindgren - RISE, Research Institutes of Sweden AB, Borås, Sweden
Johana Bernasconi - METAS, Federal Institute of Metrology, Berne-Wabern, Switzerland
Toomas Kubarsepp – METROSERT, Tallin, Estonia
Farshild Manoocheri – AALTO, Espoo, Finland

D4 deliverable of the EMPIR Joint Research Project

16NRM02 SURFACE

Title	:	Report on the intercomparison of reference materials used to measure luminance and reduced luminance coefficients of road surfaces in the laboratory and on-site software for *q* measurement uncertainty evaluation
Reference	:	EMPIR 16NRM02
Due date of the deliverable	:	November 2019
Date	:	December 2020
Dissemination level	:	CONFIDENTIAL
Author(s)	:	Paola Iacomussi- INRIM Dominique Renoux – LNE Valérie Muzet – Cerema Mikael Lindgren - RISE Johana Bernasconi – METAS Toomas Kubarsepp – METROSERT, Tallin, Estonia Farshild Manoocheri – AALTO
Keywords	:	Intercomparison on Luminance coefficient, Geometries, Reference materials, uncertainty software
Abstract	:	SURFACE had several tasks, the ones relevant for this deliverable are: • arranging a measurement intercomparison, • producing certified Reference Materials (RMs) to be used in the intercomparison and afterwards for calibrating instruments, • producing dedicated software, under open access policy, for uncertainty calculations. This deliverable presents the results of the intercomparison carried out using dedicated RM (described in D3 document) and a description of the software for uncertainty calculation. Intercomparison protocol, software guidelines and data overview are in the Appendixes. The intercomparison highlights the need of deeper investigation on the measurement model and instrument performances: as it is the first exercise on a comparison on luminance coefficient measurement capabilities, the easiest approach in the definition of measurement uncertainty was followed. The analysis of the Degree of Equivalence of the data, highlights the need of the LUMCORUN software and of a deep metrological evaluation of measuring devices. The data have a very low compatibility level even if the repeatability of the measurements of each laboratory is very high. So, the use of the standard deviation of the mean of the measurements is a poor estimator of the measurement uncertainty, and the impact of correlations among measurement geometries and instruments characteristics plays the most relevant role.
Contact	:	https://surface-nrm02.eu

About the EMPIR

The European Metrology Programme for Innovation and Research (EMPIR) coordinates research projects to address grand challenges, while supporting and developing the SI system of measurement units. There is an increased focus within EMPIR on innovation activities to target the needs of industry and accelerate the uptake of research outputs. The programmes capacity-building projects aim to bridge the gap between EU member states with emerging measurement systems and those with more developed capabilities. The EMPIR is jointly supported by the European Commission and the participating countries within the European Association of National Metrology Institutes (EURAMET e.V.). The EMPIR will ensure collaboration between National Measurement Institute, reducing duplication and increasing impact. The overall goal of the EMPIR is to accelerate innovation and competitiveness in Europe whilst continuing to provide essential support to underpin the quality of our lives.

See https://msu.euramet.org for more information

About the 16NRM02 SURFACE

SURFACE aims at providing metrological foundations for the photometric characterisation of road surfaces in order to realise lighting systems, such as smart and adaptative lighting systems. The project is a Joint Research Project coordinated by INRiM, belonging to the European Metrology Research Programme for Innovation and Research (EMPIR) of the European Metrology Association of National Metrology Institutes (EURAMET). See https://surface-nrm02.eu for more information

SUMMARY

SURFACE had several tasks, the ones relevant for this deliverable are:

- arranging a measurement intercomparison,
- producing certified Reference Materials (RMs) to be used in the intercomparison and afterwards for calibrating instruments,
- producing dedicated software, under open access policy, for uncertainty calculations.

This deliverable presents the results of the intercomparison carried out using dedicated RM (described in D3 document) and a description of the software for uncertainty calculation. Intercomparison protocol, software guidelines and data overview are in the Appendixes.

The intercomparison highlights the need of deeper investigations on the measurement model and instrument performances: as it is the first exercise on a comparison on luminance coefficient measurement capabilities, the easiest approach in the definition of measurement uncertainty was followed. The analysis of the Degree of Equivalence of the data, highlights the need of the LUMCORUN software and of a deep metrological evaluation of measuring devices. The data have a very low compatibility level even if the repeatability of the measurements of each laboratory is very high. So, the use of the standard deviation of the mean of the measurements is a poor estimator of the measurement uncertainty, and the impact of correlations among measurement geometries and instruments characteristics plays the most relevant, role.

TABLE OF CONTENTS

1 MEASUREMENT INTERCOMPARISON 4

1.1 Attendance list 4

1.2 Quantities for road reflectance characterisation 4

1.2.1 Intercomparison Quantities to measure 6

1.3 Measurement methods for *q and r* coefficient 6

1.3.1 Absolute method 6

1.3.2 Relative method 7

1.4 Measuring devices for *q and r* coefficient 7

1.4.1 Laboratory instruments to measure r-tables 7

1.4.2 Portable devices to measure r-tables 8

1.5 Samples description 8

2 LUMINANCE COEFFICIENT UNCERTAINTY EVALUATION 10

3 INTERCOMPARISON RESULTS OVERVIEW 11

3.1.1 Sample SET A figures 12

3.1.1 Sample SET B figures 16

3.2 Discussion 23

4 LUMCORUN UNCERTAINTY SOFTWARE 24

4.1 Geometrical effects 25

4.1.1 Aperture effect (regular spatial mesh) 25

4.1.2 Detector position (relative to α) (MCM) 25

4.1.3 Sample alignment in the horizontal plane (MCM) 26

4.1.4 Illumination and detection area position and overlapping (regular spatial mesh) 26

4.1.5 Illumination and detection alignment (relative to β) (MCM) 26

4.2 Examples 26

5 CONCLUSION 30

6 APPENDIX A – PECULIARITIES OF MEASURING INSTRUMENT OF INTERCOMPARISON PARTICIPANTS 31

6.1 CEREMA 31

6.2 METAS 32

6.3 IFSTTAR – UGE 33

6.4 NMF 35

6.4.1 Instrument characteristics 36

6.4.2 Stability of measurement and calibration 37

7 APPENDIX B – REFERENCE MATERIALS AND MEASUREMENT PROCEDURE OF INTERCOMPARISON PARTICIPANTS 39

7.1 Reference materials 39

7.2 Intercomparison protocol measurement procedure 40

7.3 CEREMA 41

7.3.1 Calibration procedure: 42

7.3.2 Description of the measurement uncertainty model 42

7.3.3 Additional information 42

7.3.4 Presentation of the results 42

7.3.5 Remark on the measurements 43

7.4 METAS 43

LTL-200: 43

7.4.1 Calibration procedure 44

7.4.2 Measurement uncertainties 44

7.5 IFSTTAR – UGE 44

7.5.1 UNCERTAINTY CALCULATIONS 44

7.6 NMF 45

8 APPENDIX C – PROVISIONAL DATA 46

9 REFERENCES 4

LIST OF FIGURES

Figure 1. Reference system for the measurement of *q* and *r* values: angle of observation α, lighting angles of deviation β and incidence ε. By convention, according to CIE 066 and CIE 144 guidelines and road lighting standards, for the characterisation of road photometry, α is set at 1°. 5

Figure 2: Aperture effect: Graph of relative differences % (model / integrated) using the CIE R3 27

Figure 3 Uncertainty of sample alignment: 0.2° with uniform distribution (METAS sample) 28

Figure 4 Uncertainty of detector position (α): 0.2° with uniform distribution (METAS sample) 29

Figure 5 Pictures of the Cerema gonioreflectometer with the now replaced Pritchard photometer (a), the new camera with the computer operating it (b), the different metallic holders of the camera (c) 32

Figure 6 The gonioreflectometer of Univ. Gustave Eiffel 34

Figure 7 Diagram of the gonioreflectometer 34

Figure 8 Principles of the NMF box. 36

Figure 9: A close-up of a camera image. 37

Figure 10: Built-in wedge. 38

Figure 11 Frame of samples 39

Figure 12 Samples DG210 and DK210 39

Figure 12 Samples DG000 and DK000 40

Figure 12 Samples GK210 and DG110 40

Figure 13 Picture of the sample holder device (a) and the sample positioning process thanks to the goniophotometer software 42

Figure 14 Picture of the illuminancemeter (a) and the perfect diffuser (spectralon 99%) (b) 42

LIST OF TABLES

Table 1 Intercomparison participants and measurement system used 4

Table 2 comparison of quantity equation and measurement model 10

Table 3 Values of Q0, S1 of sample SET A 12

Table 4 SET A r- values 14

Table 5SET B Q0 S1 values 17

Table 6 SET B r-values 19

Table 7 METAS Instruments characteristics 32
Table 8 Directions in which the measured values will be compared 41
Table 9 Additional observation angles 41

INTRODUCTION

Specification concerning road lighting and the photometry of road surface was established more than 40 years ago. However, pavement surface characteristics are crucial for functional quality and safety of roads, related not only to its mechanical and dynamic performance, but also to its visual performance and the safety at night of all road users. In Europe there are 5 Million kilometres of roads[1], about the 40% of them are lit, according to three different European countries Road National Administrations, by lighting systems designed considering photometric performance of pavements published in a technical documents of the 1970s[2]. Currently, road lighting installations must comply with the directives of the European Road Lighting Standards[3].

Considering the physical property of the pavement, the luminance coefficient *q* of the road links the illuminance (linearly proportional to energy consumption) with the luminance related to the visual performance, described by a vision model which defines the luminance values required to recognize obstacles on the road. The latter is not linearly linked to the energy consumption.

Designers determine the required number and spacing of road luminaires along a road to fulfil the requirements for road luminance and quality parameters values, given in the EN Standard[3] with the additional goal of energy optimization.. To do these calculations based on luminance criterion, designers use reference data of the reduced luminance coefficient *r* values (called *r-tables*), derived from q multiplied by the cube of the cosine of the angle of incidence, published in the CIE 144 document[4]. However, these *r-tables* are derived from measurements carried out more than 40 years ago and provides values only for given direction of illumination, the most relevant in road lighting.

Furthermore, measurement devices for luminance (i.e. goniophotometers) are only available in selected research institutes. These devices, although capable of producing accurate measurements, are very costly and time consuming. Some commercial portable devices have been developed by luminaire manufacturers; however they lack a clear assessment of photometric and geometrical performance. In addition, no measurement uncertainty evaluation, guidelines, or reference materials for calibration are available and no intercomparison has been realised in the last 20 years, so the traceability of these commercial devices has never been tested.

SURFACE had several tasks, the ones relevant for this deliverable are:

- arranging a measurement intercomparison,
- producing certified Reference Materials (RMs) to be used in the intercomparison and afterwards for calibrating instruments,
- producing dedicated software, under open access policy, for uncertainty calculations.

This deliverable presents the results of the intercomparison carried out using dedicated RM (described in D3 document) and a description of the software for uncertainty calculation. Intercomparison protocol, software guidelines and data overview are in the Appendixes.

1 MEASUREMENT INTERCOMPARISON

The KCDB (Key Comparison Database) has a deficiency in terms of material properties characterisation in comparison with source photometric (or radiometric) properties characterisation. In KCDB only five Key Comparisons are ascribed to material reflectance properties, all of them on diffuse reflectance, and not useful for q and *r* coefficients. When the SURFACE project was launched, only two NMI outside Europe (Australia and USA) declared CMCs (Calibration and Measurements Capabilities) on luminance coefficient, currently on NIST has a CMC on luminance coefficient but for measurement geometries (0/0, 0/45) useless in road characterisation.

The information on the luminance coefficient intercomparison has been disseminated in several ways: at conferences, during stakeholder meetings and at CIE TC4-50 meeting. In this way the information could reach all interested parties: consortium partners and stakeholders attended the intercomparison.

1.1 Attendance list

The intercomparison participants and their measurement systems are listed in Table 1

Table 1 Intercomparison participants and measurement system used

Participant Laboratory		Instrument
CEREMA	Consortium Partner	Goniophotometer
RISE	Consortium Partner	Goniophotometer
METAS	Consortium Partner	Goniophotometer
		Portable Device
IFSTTAR – Université Gustave Eiffel (UGE)	SURFACE Collaborator	Goniophotometer
NMF group	SURFACE Collaborator	Portable Device

Peculiarities of measuring instruments are listed in §6 (APPENDIX A – Peculiarities of measuring instrument of intercomparison participants).

1.2 Quantities for road reflectance characterisation

The methodology of photometrically characterising pavements was developed in the seventies[5] and updated in 1982[6] and 2001[4]. The quantities used in road lighting characterization are described in several reports from the International Commission on Illumination (CIE).[7–9]

In road photometry, the most characteristic parameter is the luminance coefficient *q*, given as:

$$q = \frac{L}{E} \qquad (1)$$

It is the ratio between the luminance *L* in cd/m², which the observer sees, and the illuminance *E* in lux which is incident on the surface. Since the eighties, for practical reasons, the luminance coefficient was replaced by the reduced luminance coefficient *r* in cd/m²/lux, which is derived from *q*:

$$r = q \cos^3 \varepsilon \qquad (2)$$

Where ε is the lighting angle of incidence, as shown in Figure 1

The standardised viewing height is 1.5 m and the angle of observation α is constant at 1°, corresponding to an observation distance of 86 m. The lighting standards use the area of the road between 60 m and 160 m ahead of the driver, because it is considered an important area for the detection of obstacles. It was also defined for interurban driving where the speed is about 80 to 90 km/h. The observation angle of 1°, is a convention, according to CIE 066 and CIE 144 guidelines and road lighting standards.

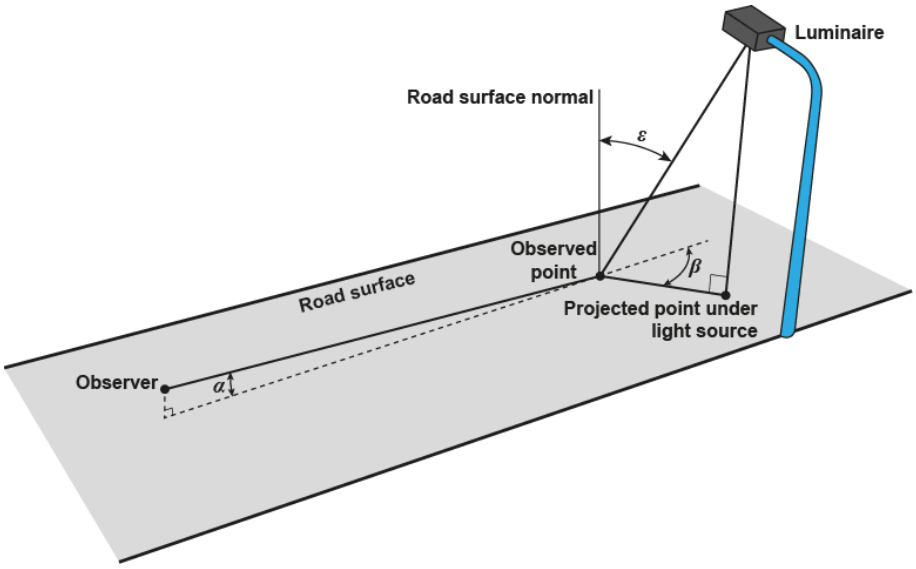

Figure 1. Reference system for the measurement of *q* and *r* values: angle of observation *α*, lighting angles of deviation *β* and incidence *ε*. By convention, according to CIE 066 and CIE 144 guidelines and road lighting standards, for the characterisation of road photometry, *α* is set at 1°.

A reduced coefficient table called *r*-table, is a table where the luminance coefficient *r* is given for a combination of fixed lighting angles *β* between 0 and 180° and tan *ε* between 0 and 12.

The average luminance coefficient Q_0, represents the degree of lightness of the measured surface[4]. It is computed as the average of the luminance coefficients over the specified solid angle, Ω_0:

$$Q_0 = \frac{1}{\Omega_0} \int q \, \mathrm{d}\Omega \qquad (3)$$

In practice, due to the finite number of measurements, the integration results in a numerical summation approximated with weighting factors corresponding to the solid angle attributed to each value $\Delta\omega$ and given for each combination of tan *ε* and *β* angles.[7]

$$Q_0 = \frac{\sum q \cdot \Delta\omega}{\sum \Delta\omega} \qquad (4)$$

The specular factor S_1 represents the degree of specularity (shininess) of the observed surface. It is defined as the ratio between the reduced luminance coefficients at two specific illumination conditions:

$$S_1 = \frac{r(\beta=0, \tan\varepsilon=2)}{r(\beta=0, \tan\varepsilon=0)} \qquad (5)$$

1.2.1 Intercomparison Quantities to measure

The quantities to measure in the SURFACE intercomparison are:

- Reduced luminance coefficient, *r*
- Q0 and S_1 values

At least three measurements of each artefact and for each measuring geometry must be carried out, which means taking out the reference material before the next measurement.

The reduced luminance coefficient and Q0 and S1 values of the artefacts must be measured following the measuring procedure of each laboratory for the given observation angles.

The intercomparison exercise is to measure the full r-table of all artefacts, or, since not all measuring devices are able to measure all tanε and β lighting angles as reported in Table 3 of EN 13201-3, at least for all measuring directions of the instrument and (if possible) for the directions at which the values will compared (see §) and for α=1° of observation.

If the measuring instrument is able to measure additional and/or non-conventional directions it is request to measure the samples also in the additional directions (in Table 8 and for the SURFACE additional observation angles in Table 9).

The values to record for each sample, including flat samples, are:

- the measured r values of of three measurements in the direction as specified in §4.2
- the Q0, S1 values
- the measurement uncertainty (or the calculated standard deviation following the laboratory procedure) of r-values and Q0, S1.

For each RM sample measured data have to be recorded in a dedicated excel file:

- Measured r-table values of each sample, if not possible to provide the full r-table refer to §4.2 for accepted/requested geometries. Please remember that measured values will be compared for directions as in Table 8, with observation angle 1°, additional directions are listed inTable 9.
- If available, the measurement uncertainty value on measured values
- The environmental measuring conditions

1.3 Measurement methods for *q and r* coefficient

As stated in Deliverable 5 (Pre-normative guidelines for measurement methods and procedures), there are basically two approaches to measure the luminance coefficient and subsequently *r* coefficient.

1.3.1 Absolute method

The definition of the luminance coefficient is directly applied. Thus, the luminance coefficient of a test surface $q = \frac{L}{E}$. In terms of measured signals

$$q = \frac{s_L}{s_E} \cdot \frac{k_E}{k_L}, \quad (1)$$

where s_L is the signal measured by the luminance detector when measuring the test surface, s_E is the signal of the illuminance detector, k_E is the sensitivity of the illuminance detector obtained by calibration, and k_L is the sensitivity of the luminance detector obtained by calibration. In this case, the luminance and illuminance

detector each need to be calibrated separately, following a standard procedure. It could be noted here that the illuminance can be measured once, for the normal incidence, and then deduced for other incidence angles applying the cos (**ε**) law and optionally monitoring the light source.

1.3.2 Relative method

A reflection standard (reference surface R) of known luminance coefficient q_R is used to calibrate the system. In addition, often an additional detector is used to monitor the signal of the source, because the measurement is performed in two different times, one to calibrate the instrument with the standard, and one for the actual sample measurement :

$$q_T = q_R \frac{s_{L,T}}{s_{L,R}} \cdot \frac{s_{M,R}}{s_{M,T}}, \quad (2)$$

where $s_{L,T}$ is the signal of the (luminance) detector when measuring the sample surface, $s_{L,T}$ is the signal of the (luminance) detector when measuring the reference surface of the standard, $s_{M,R}$ is the signal of the monitor detector of the source when measuring the reference surface of the standard, $s_{M,T}$ is the signal of the monitor detector of the source when measuring the sample surface, and q_R is the luminance coefficient of the reference surface. In this case, the reference surface needs to be measured by an accredited laboratory. The linearity of the detector also needs to be known through calibration.

Ideally, multiple measurements of the same sample should be made. Obviously, the feasibility depends a lot on the time needed for one measurement. It is recommended to measure at least twice. It is also recommended to start the measurement with a standard plate to ensure that the alignment of the setup and the measurement conditions are normal.

1.4 Measuring devices for *q and r* coefficient

In order to evaluate the current state of the art of road surface photometry, a review of existing devices was done in Deliverable 1 (Report on photometric quantities for road surface materials to support EN 13201 reference tables). The devices used to measure the surface reflection property, and more specifically the luminance coefficients, can be classified into two main subsets:

- laboratory instruments, which are used to make absolute measurements of *r*-tables and can serve as a reference devices.
- portable devices, which are used to measure the road surface *in situ* and provide a relative measurement.

1.4.1 Laboratory instruments to measure r-tables

Laboratory instruments consist of a light source, a sample holder and a detector to measure the luminance. The geometry is usually designed to cover the different illumination angles defined in the *r*-table. Most of them are fully automated, which makes it easier to measure all the illumination positions. The detection needs to take into account the $V(\lambda)$ curve[10] in order to measure the luminance. The illuminance on the surface depends on the illumination angle **ε** and can be measured using a luxmeter. A review of the actual laboratory measuring devices was done in the SURFACE project and is published in [11].

Laboratory setups are typically characterized by a large distance between the source and the sample (1 to 5 m), which results in good collimation angles (below 1° for most instruments), limiting the uncertainty on the illumination angle. The detector is often placed at a distance such that the acceptance angle of the detection is small.

They usually allow the measurement of the full *r*-table, at the cost of longer measurement times (from 30 minutes to several hours). For most of them, it is therefore possible to compute Q_0 directly using the weighting factor given in[7] which corresponds to the numerical integration over the considered solid angle. Some of them rely on interpolation or extrapolation.

These devices are expected to have relatively small measurement uncertainty, typically evaluated to be around 10 %.[12–14] They are therefore used to make the reference measurements necessary to calibrate the portable devices. However, a uniform approach is currently lacking regarding the calibration methodology, the measurement procedure, the traceability, and the measurement uncertainty of these instruments. These shortcomings will be addressed by the SURFACE project in a subsequent contribution.

The main disadvantage of laboratory instruments is that they require samples to be extracted from the road, which is destructive and costly. For this reason, laboratory systems are not suitable to follow the evolution of road surface reflectance over time, and do not allow multiple measurements in the exact same spot throughout several years. They are also poorly suited for studying different parts of the road.

1.4.2 Portable devices to measure *r*-tables

Portable devices are setups that can be transported and used for *in-situ* measurements. Usually, they fit in a car and one or two persons are needed to carry and install them. This results in strict requirements in terms of size and weight, which limits the solutions. A review of the actual portable measuring devices was done in the SURFACE project and is published in [11].

These devices always contain some compromises on the measurements, either with restricted measurement geometry combinations, or with larger measurement uncertainties. The solutions adopted are very varied in their mechanical and optical solutions. Some devices measure using pre-determined illumination angle configurations.[15–18] Other devices measure the full *r*-table but face other issues, like the restricted size, which makes it more difficult to obtain a highly collimated source.[19,20]

Using restricted geometry combinations, the setup does not measure the full *r*-table. Only selected illumination angles (ε, β) are used in the measurement. These devices usually allow the measurement of the specular components directly, but not Q_0. Some modelling, interpolation, and extrapolation are then used to retrieve the complete *r*-table and to compute Q_0.[15] Sometimes, the measured data or the resulting modelled *r*-tables are used to find the closest measured *r*-table from a database based on measurements done with a laboratory instrument.[16] This approach avoids the discrepancies found between standard CIE *r*-tables, which were done on old pavement surfaces, and measurements done on roads with more recent pavement. However, it assumes that the characteristics of particular pavements are present in the database used. This shows the importance of having up to date reference *r*-tables, which are representative of the current road surfaces, because some portable devices rely heavily on databases for their interpolation model for example.

The main advantage of portable devices is that they allow non-destructive measurements. This means that the evolution of pavements can be studied over a long period of time[21,22] and that this information can be used to make lighting more efficient, by planning a well-suited lighting solution and by using dynamic adaptive lighting.[23] Portable devices can evaluate the heterogeneity of the photometric characteristics of the road surface and, for example, make many measurements on the wheel and central parts of a lane. Therefore, despite of being generally less precise, they are more representative of the actual road photometry.

1.5 Samples description

The comparison pack consists of box with several artefacts:

- 1 Artefact square flat of 20 cm by 20 cm in printed grey - matte
- 1 Artefact square flat of 20 cm by 20 cm in printed black - matte

- 1 Artefact square flat of 20 cm by 20 cm in printed black - glossy
- 1 Wrought artefact with random point of size range 6 to 10 mm, high range 5 to 10 mm, 20% of flat surfaces printed in grey - matte
- 1 Wrought artefact with random point of size range 6 to 10 mm, high range 5 to 7 mm, 20% of flat surfaces printed in grey - matte
- 1 Wrought artefact with random point of size range 6 to 10 mm, high range 5 to 7 mm, 20% of flat surfaces printed in black - matte
- 1 Wrought artefact with random point of size range 6 to 10 mm, high range 5 to 7 mm, 20% of flat surfaces printed in black – glossy

All artefacts are IoT products: 3D printed artefact specifically designed Reference Material (RM) for the intercomparison as stated in Deliverable 3 (Specification document for using Reference Materials to establish traceability and evaluate measurement uncertainty for instruments used to measure luminance and reduced luminance coefficients of road surfaces).

Furthermore, the comparison pack is composed of two RM sets:

- SET A: a set of flat RM samples in matte grey, matte black, glossy black;
- SET B: a set of RM samples designed by road attributes chosen in agreement with the consortium (ref. D3 for detailed description), made in matte grey, matte black, glossy black.

SET A is a set of diffusing flat samples that will highlight linearity behaviour of instruments: expected discrepancies in the measurements will be related to linearity or severe calibration, including geometry issues.

SET B is a set of samples with geometrical attributes similar to road surface: a large height range will highlight discrepancies in the angular resolution of instruments, measuring area, and calibration.

Pictures and draws of the samples are in the appendix.

2 LUMINANCE COEFFICIENT UNCERTAINTY EVALUATION

The main document for the measurement uncertainty evaluation Guide to the expression of uncertainty in measurements (GUM) presents a very detailed approach to measurement uncertainty evaluation that could be very difficult to understand and apply in Industrial applications, mainly because the difficulties in the definition of the full equation of the measurement model. The GUM approach is the definition of a full measurement model that is not the simple expression of the quantity but is a complex expression that takes in account of measured values and of measurement procedure (Table 2 shows a simple example for the luminance coefficient measured with a relative method).

Table 2 comparison of quantity equation and measurement model

Expression of the quantity	Simplified measurement model (relative method)
$q = \frac{L}{E}$	$q_{\mathrm{T}} = q_{\mathrm{R}} \frac{s_{\mathrm{L,T}}}{s_{\mathrm{L,R}}} \cdot \frac{s_{\mathrm{M,R}}}{s_{\mathrm{M,T}}}$

To define a full measurement model, it is necessary to start from the expression of the measured quantity and introduce all possible influence parameters contributions. Usually, these contributions belong to two different families: those related to the set-up (consisting in measurement method, procedure and measuring device) and those related to the specimen. And for all of them is necessary to define their uncertainties and reciprocal correlations. Especially, this last evaluation is very challenging and is not a simple solution. If the full knowledge of the correlations among all uncertainties and of their reciprocal impact is not easily achievable, the GUM suggests to perform simulation (usually a Monte Carlo simulation) of the whole impact of the different uncertainties. A dedicated software (called LUMCORUN) was provided during our SURFACE project and described in §4.

From the laboratory point of view the measurement uncertainty could be described as composed by two contributions:

- the measurement system metrological characteristics and measurement procedures,
- the influence of the measured specimen characteristics.

When the influence parameters in the uncertainty budget are considered, it is useful to separate these two contributions because:

- the sample influence could change dramatically from one specimen to another, while the laboratory influence could remain substantially constant;
- their quantitative evaluation should suggest improvement in the measurement procedure, new layout of the measurement system and optimisation of cost.

For the SURFACE intercomparison, participants have to calculate their own uncertainty budget. Since this is the first intercomparison on the subject and nor agreed nor tested uncertainty evaluation approach is available, intercomparison participants agreed to consider the measurements dispersion (standard deviation of the different trials) as first rough uncertainty estimator, and only for laboratories able to do their own uncertainty budget, the stated uncertainty was used. With a stable version of LUMCORUN software for luminance coefficient uncertainty calculation, attending laboratories will provide calculated uncertainty values too.

3 INTERCOMPARISON RESULTS OVERVIEW

As agreed by the intercomparison participants, only measured data at given directions will be compared.

Since this is the first intercomparison on the subject, no CCPR Guidelines is available, intercomparison participants, during a dedicated virtual meeting agreed on the following approach to measurement data evaluation and Key Comparison Reference Value (KCRV) estimation:

- Since the intercomparison was a circular one, the reference value of the intercomparison was agreed by participant as the arithmetic mean of the value.
- Each participant is identified with a confidential code for r-table values and a different confidential code for integral values.
- Participant should provide, if available, U_{soft} U_{stdev} U_{lab}, where: U_{soft} is the uncertainty calculated with LUMCORUN software, U_{stdev} is the standard deviation of the measurements, U_{lab} is the value of uncertainty of the laboratory.
- If the KCRV is the aritmetic mean, the uncertainty in the Degrees of Equivalence (DoE, d_i) of each laboratory is calculated as the standard deviation of the mean considering the laboratory uncertainty provided by the participants and the uncertainty of the reference value[24].

KCRV estimator	Reference value, x_{ref}	Reference value uncertainty, $u(x_{ref})$	DoE: d_i and $u(d_i)$
Arithmetic mean of the *N* measured values	$x_{ref} = \frac{1}{N}\sum_{i=1}^{N} x_i$	$u(x_{ref}) = \sqrt{\sum_{i=1}^{N} \frac{(x_i - x_{ref})^2}{N(N-1)}}$	$d_i = x_i - x_{ref}$ $u^2(d_i) = u^2(x_i) + u^2(x_{ref})$ eq. A $u^2(d_i) = u^2(x_i) + u^2(x_{ref}) + 2u(x_i)u(x_{ref})r\left(\frac{u(x_i, x_{ref})}{u(x_i)u(x_{ref})}\right)$ eq. B

It is to note:

- Participant laboratory made N=3 measurements of every sample.
- The intercomparison value of a participant is the mathematical mean of the N measurements carried out
- Participant calculated the standard deviation of their values, weighting the discrepancies from the mean by the value N-1
- The uncertainty associated with the mathematical mean is calculated as:

$$u(\bar{x}) = \sqrt{\sum_{i=1}^{N} \frac{(x_i - \bar{x})^2}{N(N-1)}}$$

- Since there are several outliers, the associated laboratory values are not taken in account in the KCRV x_{ref} calculations and the mathematical mean for KCRV was calculated based only on values of 3 (for integral values, Q0 S1, 4) laboratories
- The uncertainty associated with the DoE d_i is calculated using eq. A if the laboratory value is not used in the x_{ref} calculations, while eq. B if the laboratory value is used in the x_{ref} calculations. Eq. B takes in account of the correlations that cannot be neglected because the limited number of trials (only 3).

A measurement is discrepant if:

$$|d_i| > 2u(d_i)$$

In appendix provisional data tables.

The following tables show the data, organized by samples set and β angle.

3.1.1 Sample SET A figures

Samples of SET A are flat samples. Their behavior is not representative of road surface behavior but are useful to identify discrepancies due to linearity and alignment (especially sample GK000) of the measuring system and calculations of r values.

Table 3 Values of Q0, S1 of sample SET A

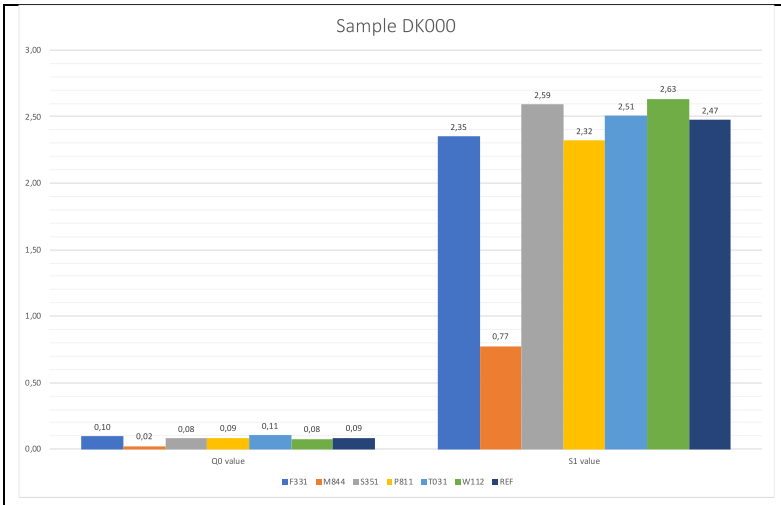

F331 u(Q0)= 0,0003 u(s1)=0,03
M844 u(Q0)= 0,01 u(s1)=0,25
S351 u(Q0)= 0,0002 u(s1)=0,021
P811 u(Q0)= 0,0002 u(s1)=0,016
T031 u(Q0)= 0,002 u(s1)=0,15
W112 u(Q0)= 0,001 u(s1)=0,01
REF u(Q0)= 0,001 u(s1)=0,01

Value KCRV using F331, S351, P811, W112			
Q0 value	0,09	u (Q0)	0,002
S1 value	2,47	u (S1)	0,72

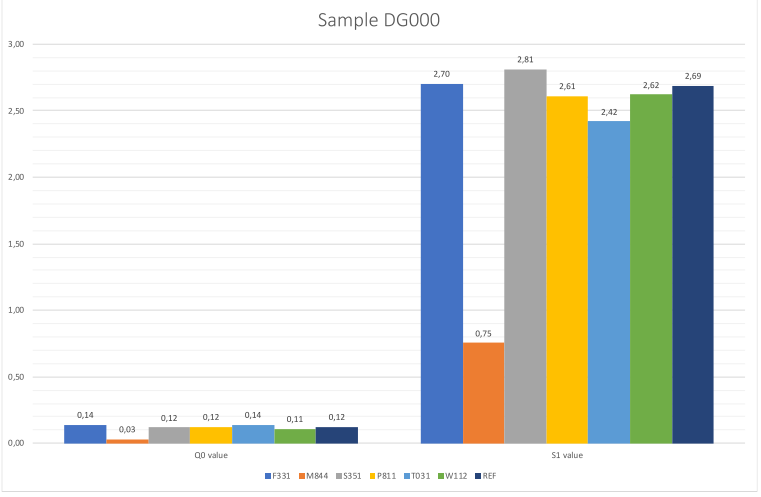

F331 u(Q0)= 0,002 u(s1)=0,03
M844 u(Q0)= 0,01 u(s1)=0,27
S351 u(Q0)= 0,0009 u(s1)=0,007
P811 u(Q0)= 0,001 u(s1)=0,01
T031 u(Q0)= 0,002 u(s1)=0,10
W112 u(Q0)= 0,001 u(s1)=

Value KCRV using F331, S351, P811, W112			
Q0 value	0,12	u (Q0)	0,003
S1 value	2,69	u (S1)	0,77

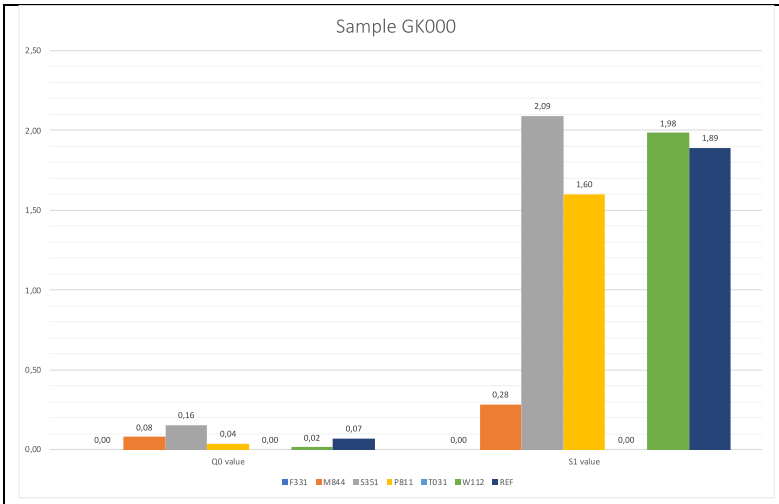

F331
M844 u(Q0)= 0,023 u(s1)=0,014
S351 u(Q0)= 0,0009 u(s1)=0,007
P811 u(Q0)= 0,0005 u(s1)=0,011
T031 u(Q0)= 0,002 u(s1)=0,010
W112 u(Q0)= 0,001 u(s1)=

Table 4 SET A r- values

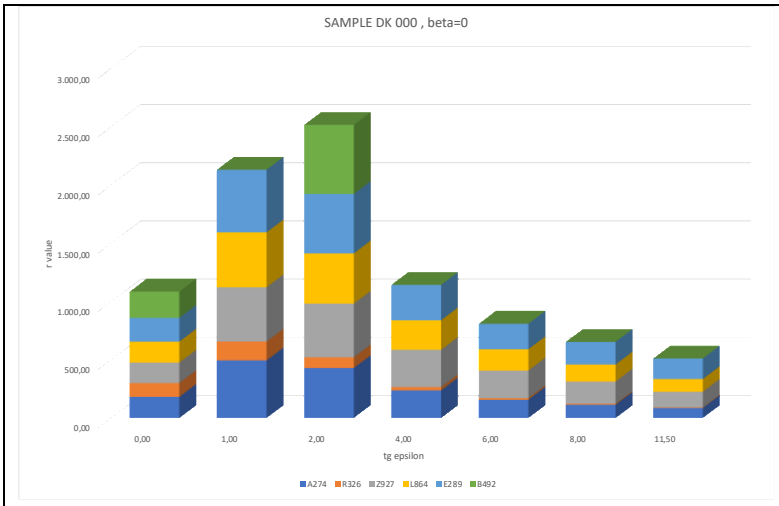

KCRV using A274, Z927 L864			
	b		
tg e	0,00	15,00	30,00
0,00	179,74	179,69	180,48
1,00	477,95	386,46	223,14
2,00	441,18	205,84	64,82
4,00	271,00	44,43	13,75
6,00	192,82	18,31	5,90
8,00	150,89	10,23	#DIV/0!
11,50	110,56	5,05	#DIV/0!

UNC - KCRV using A274, Z927 L864			
	b		
tg e	0,00	15,00	30,00
0,00	1,32	1,31	1,25
1,00	5,00	5,65	2,74
2,00	5,00	5,36	1,12
4,00	12,35	1,65	0,25
6,00	11,43	0,91	0,10
8,00	10,86	0,57	#DIV/0!
11,50	7,31	0,23	#DIV/0!

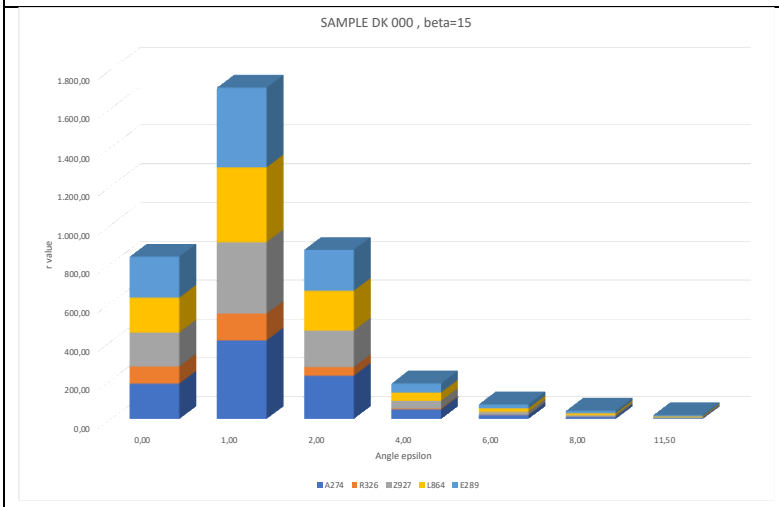

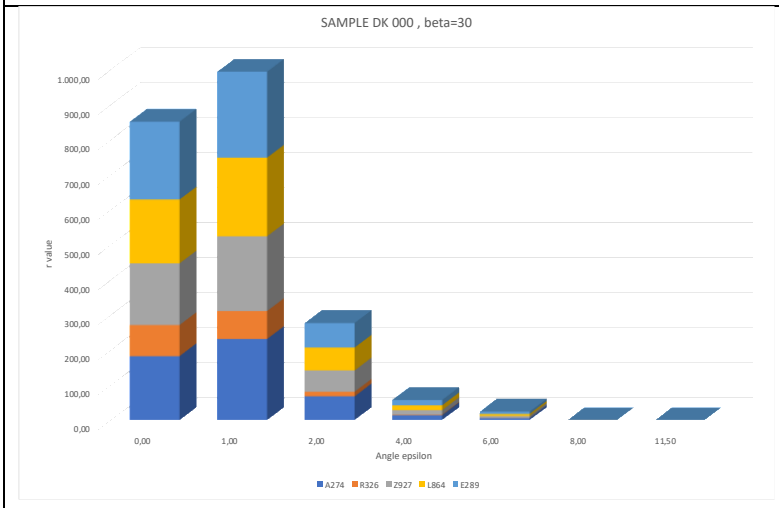

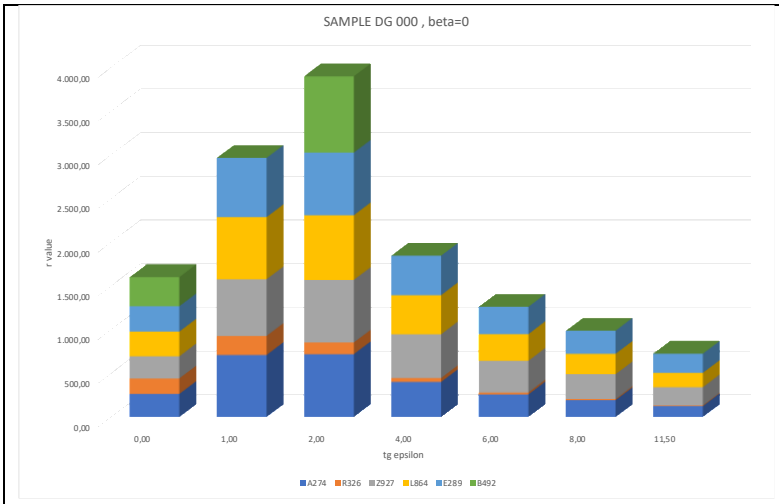

KCRV using A274, Z927 L864			
	b		
tg e	0,00	15,00	30,00
0,00	267,86	266,50	266,35
1,00	691,12	498,96	278,03
2,00	726,01	249,65	85,64
4,00	450,86	54,89	20,63
6,00	310,03	25,35	9,04
8,00	237,80	14,63	#DIV/0!
11,50	167,02	7,68	#DIV/0!

UNC - KCRV using A274, Z927 L864			
	b		
tg e	0,00	15,00	30,00
0,00	4,35	4,08	4,05
1,00	10,83	9,54	4,26
2,00	3,92	8,64	1,10
4,00	13,80	1,58	0,13
6,00	14,61	1,18	0,03
8,00	12,62	0,67	#DIV/0!
11,50	11,68	0,24	#DIV/0!

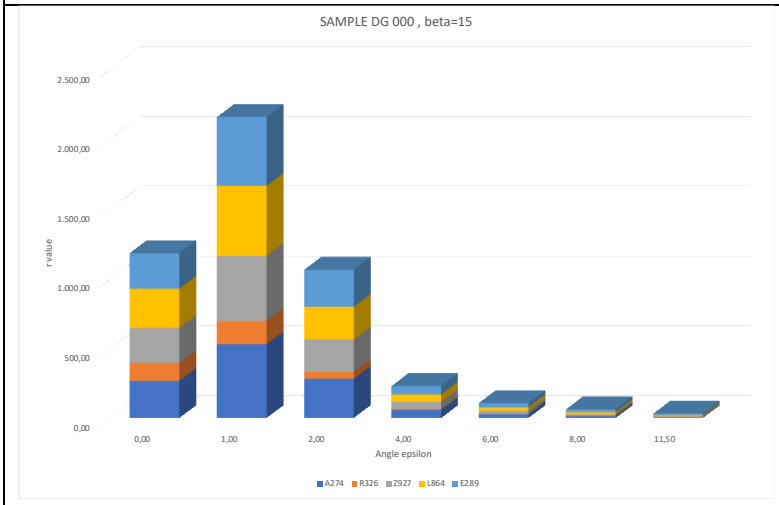

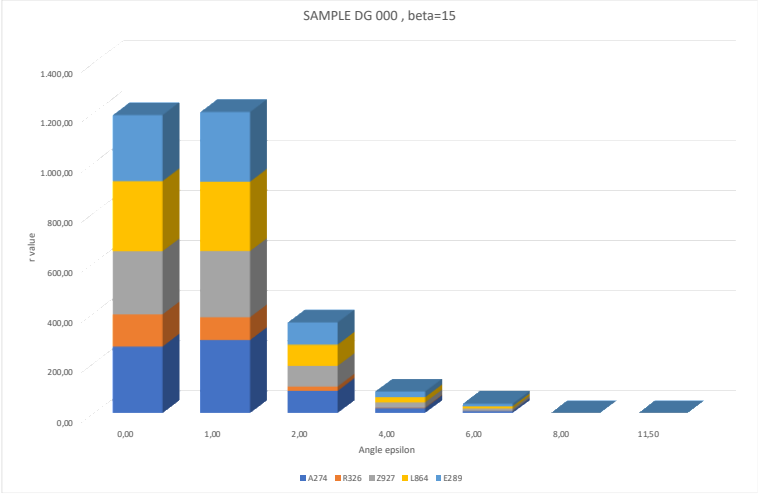

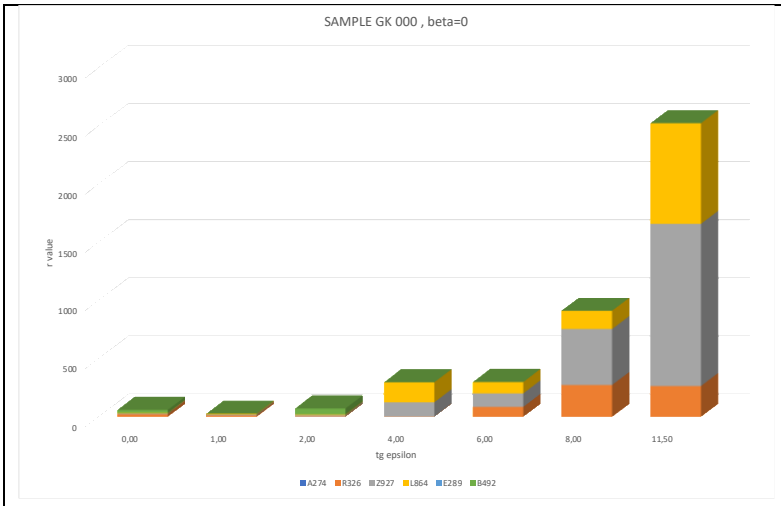

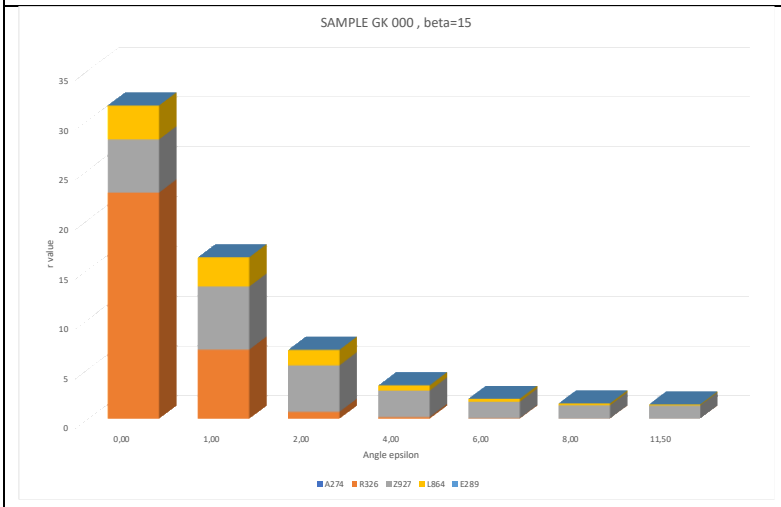

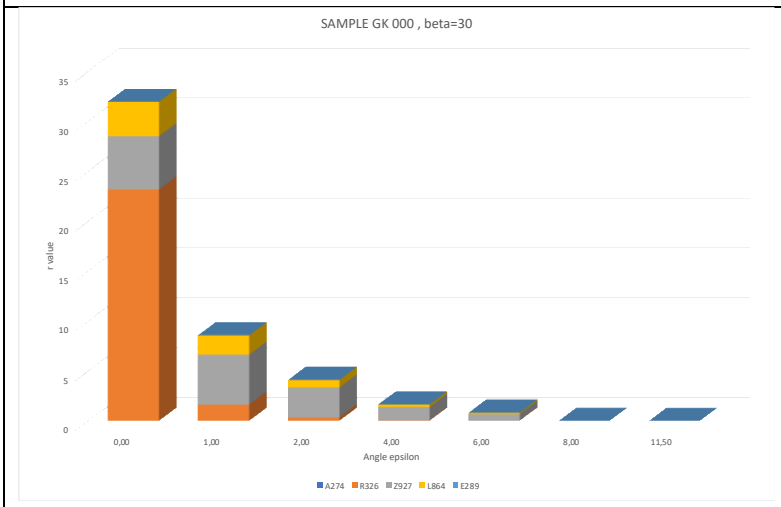

3.1.1 Sample SET B figures

Samples of SET B are samples with several irregular solid shapes to figure the peculiarities of road surfaces. Even if their photometric behavior is not representative of given reference road surface (like CIE reference r-

tables), their peculiarities mimic the physical properties of road surface with a diffusive and specular behavior, solid shapes providing a rough surface with shadowing effects.

Table 5SET B Q0 S1 values

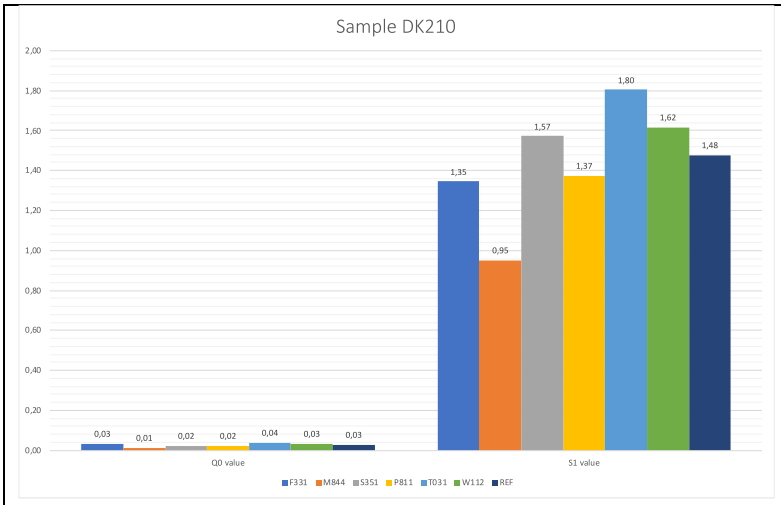

F331 u(Q0)= 0,0006 u(s1)=0,02
M844 u(Q0)= 0,003 u(s1)=0,36
S351 u(Q0)= 0,0002 u(s1)=0,008
P811 u(Q0)= 0,0003 u(s1)=0,09
T031 u(Q0)= 0,001 u(s1)=0,09
W112 u(Q0)= 0,00 u(s1)=0,05

Value KCRV using F331, S351, P811, W112			
Q0 value	0,03	u (Q0)	0,002
S1 value	1,48	u (S1)	0,44

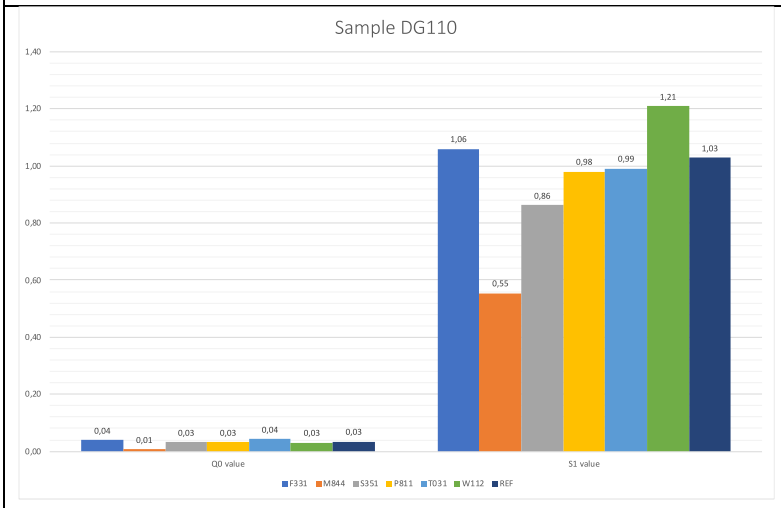

F331 u(Q0)= 0,00u(s1)=0,015
M844 u(Q0)= 0,0002 u(s1)=0,011
S351 u(Q0)= 0,0002 u(s1)=0,0044
P811 u(Q0)= 0,0003 u(s1)=0,054
T031 u(Q0)= 0,0008 u(s1)=0,048
W112 u(Q0)= 0,001 u(s1)=0,05

Value KCRV using F331, S351, P811, W112			
Q0 value	0,03	u (Q0)	0,001
S1 value	1,03	u (S1)	0,30

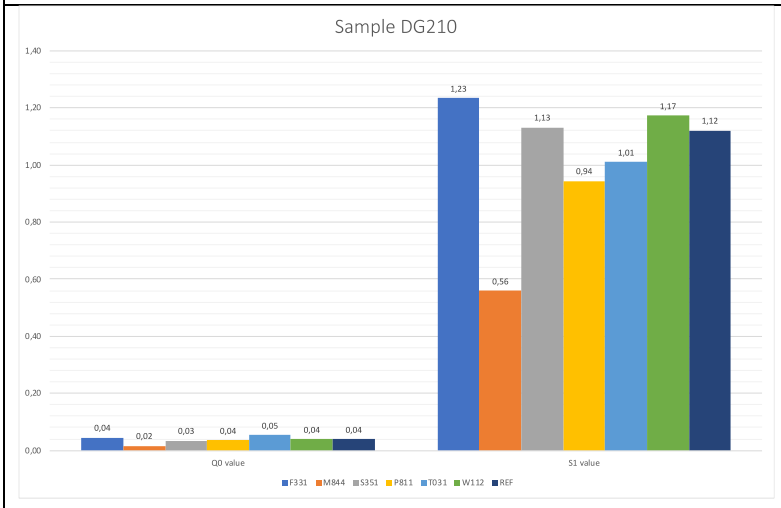

F331 u(Q0)= 0,001 u(s1)=0,01
M844 u(Q0)= 0,004 u(s1)=0,19
S351 u(Q0)= 0,0003 u(s1)=0,01
P811 u(Q0)= 0,0002 u(s1)=0,09
T031 u(Q0)= 0,001 u(s1)=0,05
W112 u(Q0)= 0,001 u(s1)=0,04

Value KCRV using F331, S351, P811, W112			
Q0 value	0,04	u (Q0)	0,003
S1 value	1,12	u (S1)	0,31

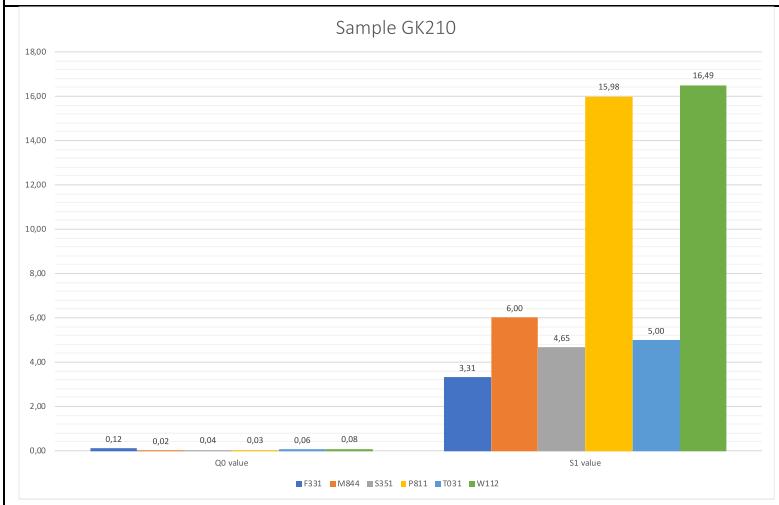

F331 u(Q0)= 0,002 u(s1)=1,29
M844 u(Q0)= 0,004 u(s1)=0,18
S351 u(Q0)= 0,0001 u(s1)=0,30
P811 u(Q0)= 0,001 u(s1)=3,0
T031 u(Q0)= 0,009 u(s1)=0,29
W112 u(Q0)= 0,002 u(s1)=1,54

Table 6 SET B r-values

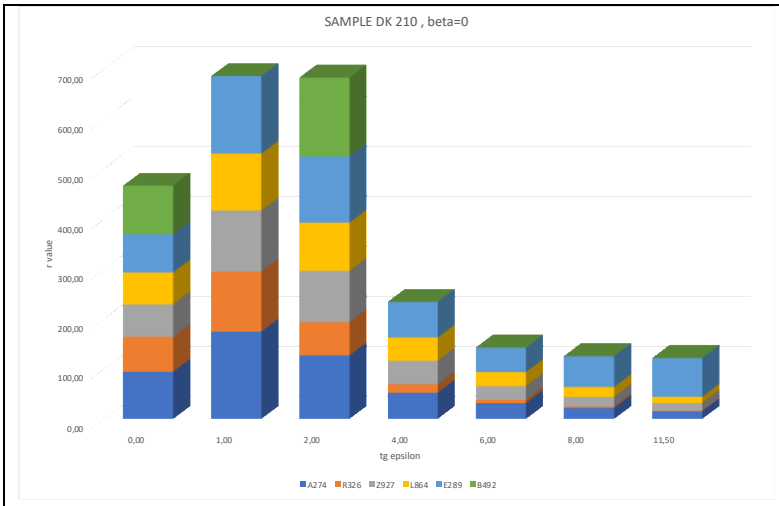

KCRV using A274, Z927 L864			
	b		
tg e	0,00	15,00	30,00
0,00	74,54	74,03	75,03
1,00	137,03	107,60	68,77
2,00	108,82	50,99	19,40
4,00	48,79	7,32	4,22
6,00	29,30	2,89	1,86
8,00	20,69	1,40	0,00
11,50	14,66	0,67	0,00

UNC - KCRV using A274, Z927 L864			
	b		
tg e	0,00	15,00	30,00
0,00	5,12	4,97	4,81
1,00	9,84	7,18	4,84
2,00	4,90	4,67	1,61
4,00	1,37	0,68	0,39
6,00	0,92	0,24	0,23
8,00	0,68	0,20	0,00
11,50	0,65	0,17	0,00

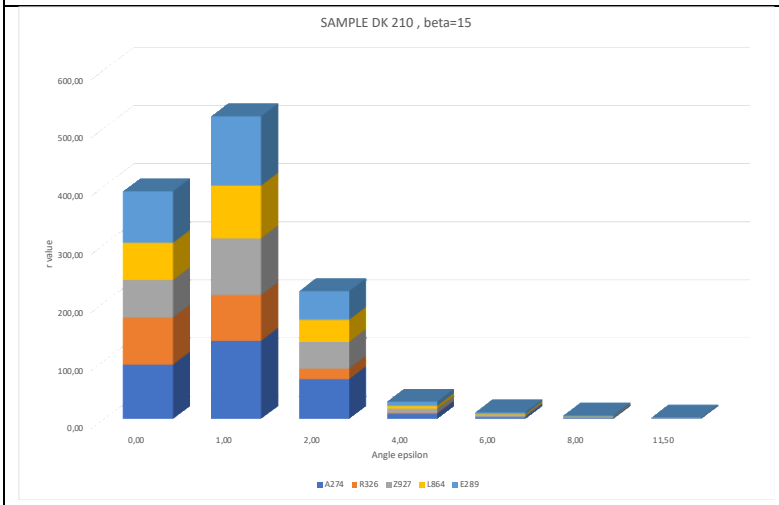

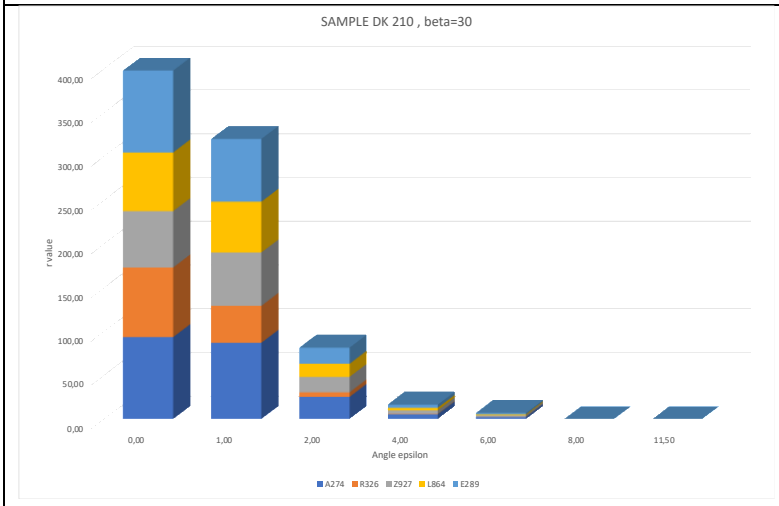

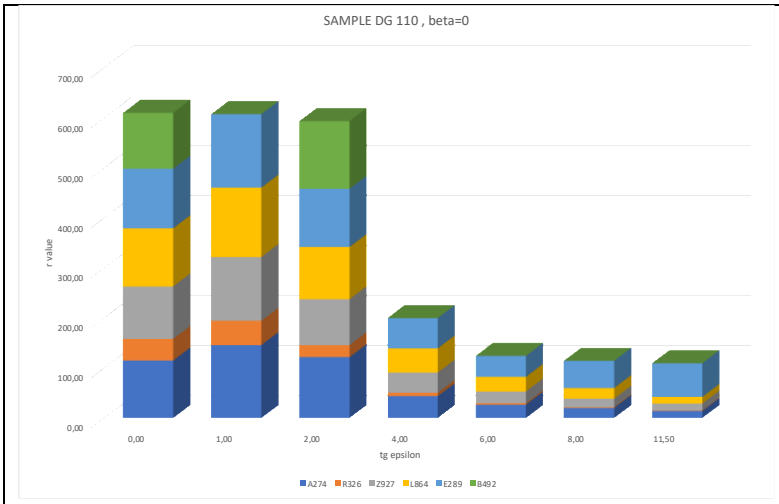

KCRV using A274, Z927 L864			
	b		
tg e	0,00	15,00	30,00
0,00	112,12	107,96	106,01
1,00	137,37	111,45	78,92
2,00	106,11	50,58	24,87
4,00	44,28	8,54	5,98
6,00	26,60	3,01	2,58
8,00	19,55	1,56	#DIV/0!
11,50	13,86	0,94	#DIV/0!

UNC - KCRV using A274, Z927 L864			
	b		
tg e	0,00	15,00	30,00
0,00	2,06	2,16	2,65
1,00	3,40	3,32	2,95
2,00	4,71	3,03	1,13
4,00	1,40	0,48	0,30
6,00	0,96	0,20	0,18
8,00	0,80	0,15	#DIV/0!
11,50	0,39	0,02	#DIV/0!

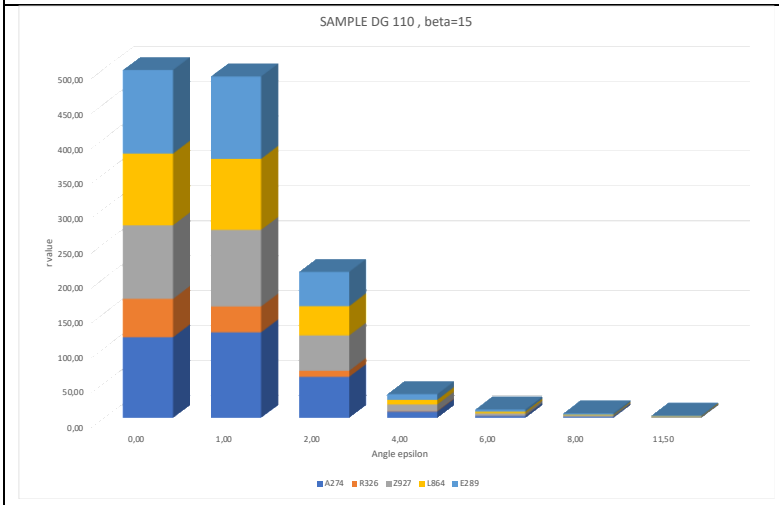

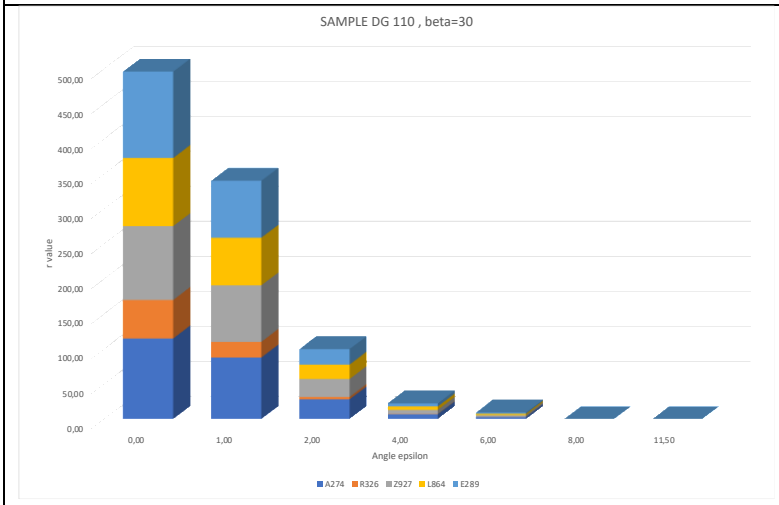

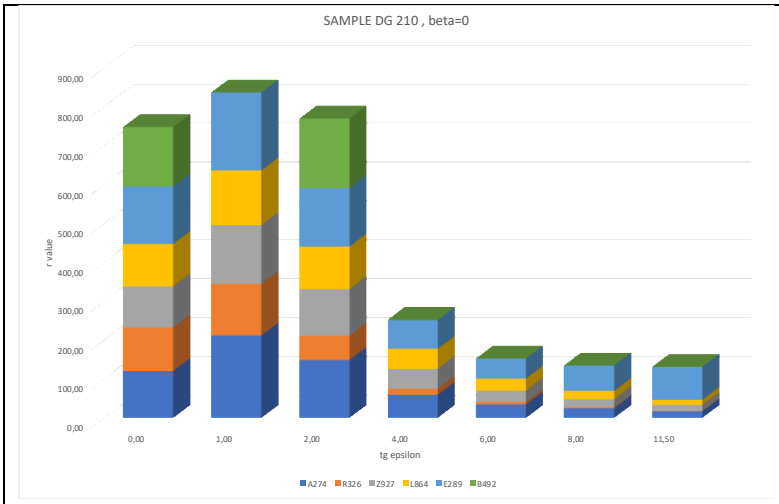

KCRV using A274, Z927 L864			
	b		
tg e	0,00	15,00	30,00
0,00	112,02	111,10	111,88
1,00	168,14	141,31	94,73
2,00	126,23	65,90	30,26
4,00	54,27	11,61	7,13
6,00	31,86	4,59	3,23
8,00	22,68	2,50	#DIV/0!
11,50	15,36	1,25	#DIV/0!

UNC - KCRV using A274, Z927 L864			
	b		
tg e	0,00	15,00	30,00
0,00	13,40	13,27	13,42
1,00	22,22	18,50	11,67
2,00	15,93	8,85	3,75
4,00	6,67	1,50	0,89
6,00	3,94	0,58	0,39
8,00	2,83	0,34	#DIV/0!
11,50	1,98	0,17	#DIV/0!

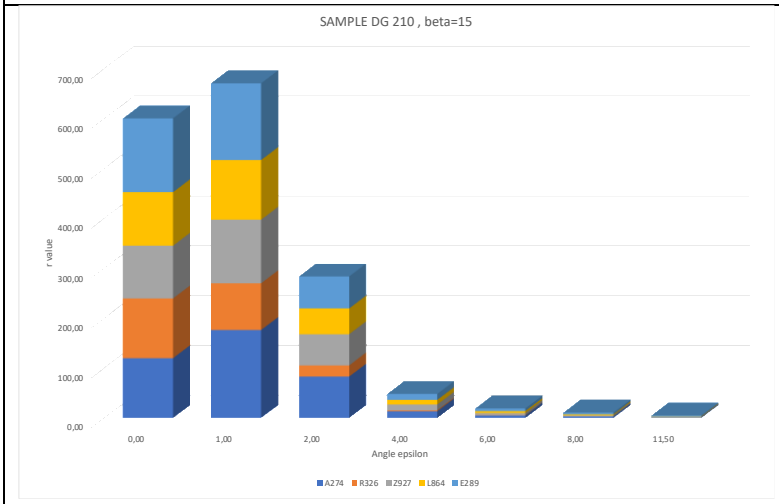

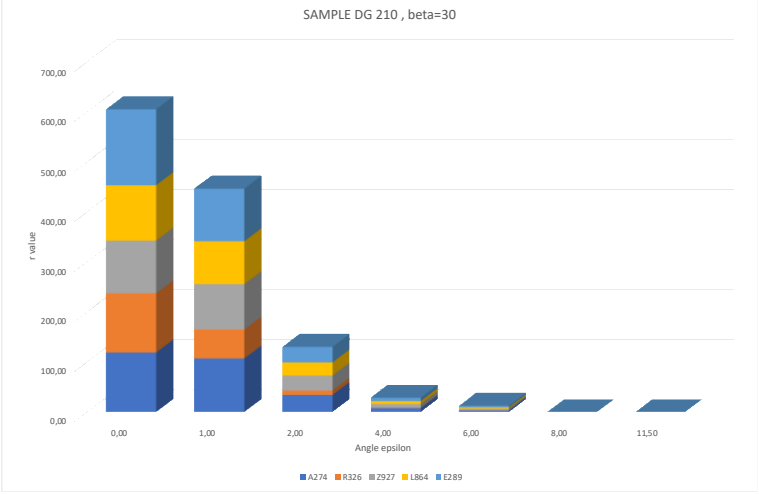

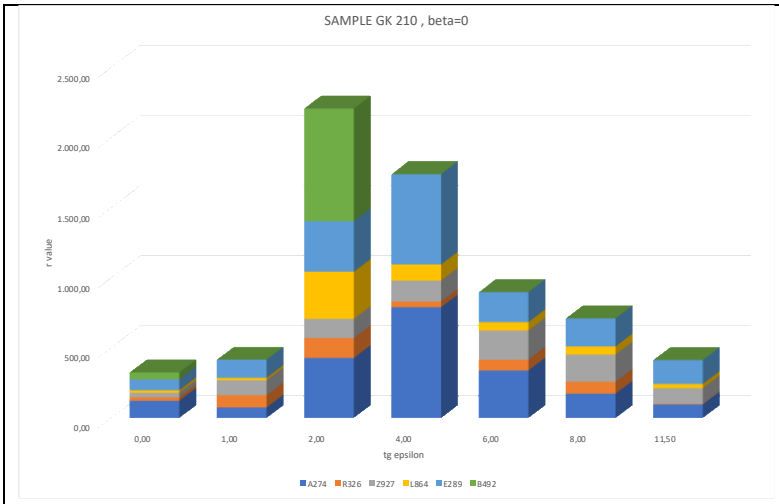
SAMPLE GK 210 , beta=0
r value
2.500,00
2.000,00
1.500,00
1.000,00
500,00
0,00
0,00
1,00
2,00
4,00
6,00
8,00
11,50
tg epsilon
A274 R326 Z927 L864 E289 B492

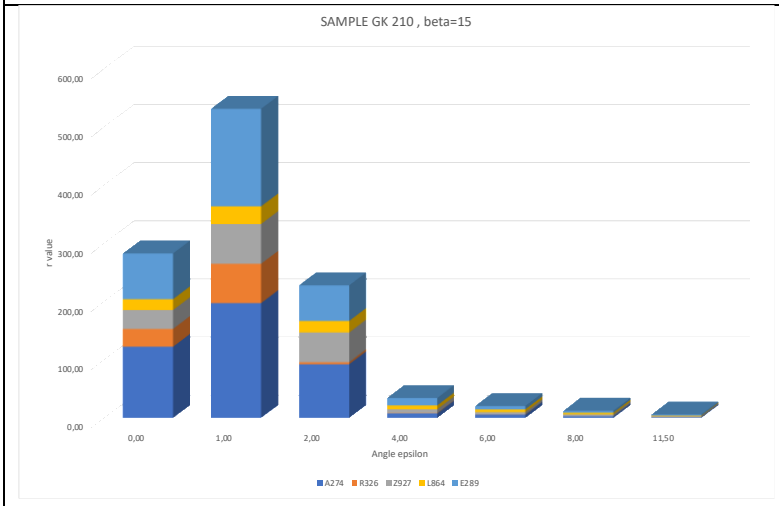
SAMPLE GK 210 , beta=15
r value
600,00
500,00
400,00
300,00
200,00
100,00
0,00
0,00
1,00
2,00
4,00
6,00
8,00
11,50
Angle epsilon
A274 R326 Z927 L864 E289

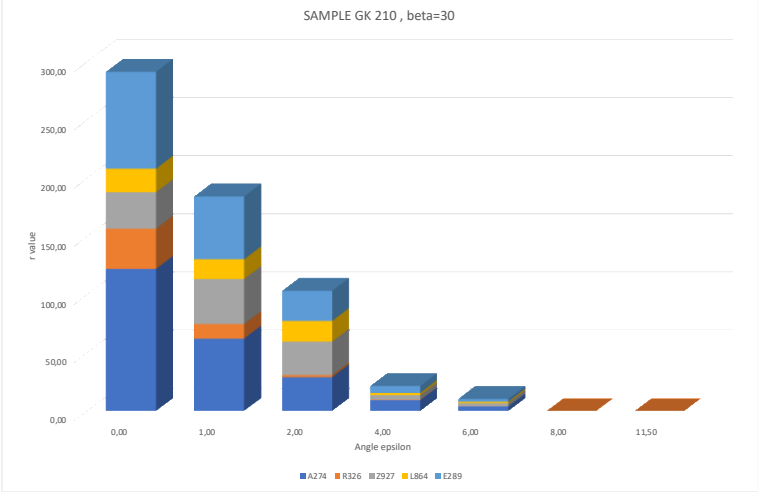
SAMPLE GK 210 , beta=30
r value
300,00
250,00
200,00
150,00
100,00
50,00
0,00
0,00
1,00
2,00
4,00
6,00
8,00
11,50
Angle epsilon
A274 R326 Z927 L864 E289

3.2 Discussion

Provisional data highlights several problems in the exercise:

- Even in SET A there are outliers, with discrepancies larger than 100%, greatest difficulties are with Glossy black sample
- Also in SET B there are outliers because of: single measurement value, systematic behaviour of laboratories
- The degree of equivalence of all measurements is very low, better agreement is reached with grey samples
- The standard deviation of the measurements is not representative of the measurement uncertainty and is either an under-estimation or a mis-estimation.
    - Measurement devices showed good repeatability (all participant have low standard deviations)
    - The RM design ensured also high position and alignment repeatability.
    - The under/misestimation of the uncertainty involves problems in the approach to the definition of KCRV and consequently in degree of equivalence of the data
- As some measurements are outliers, the KCRV can be established relying only on few data. In few cases the results seem to belong to different populations: the choice of KCRV as arithmetic mean is weak it could be of interest to investigate the impact of considering just one laboratory as reference
- Some geometrical conditions shown good data agreement among the labs, while, in the larger part of geometries, discrepancies are relevant (in few cases more than 100%) to support the need of deeper investigations. Suggested field of investigations:
    - Impact of geometries, apertures and acceptance area and eventually calibration and calculation models
    - Need of systematic corrections for given instruments and/or given measurement directions
- LUMCORUN software can help investigating the above issues providing a better understanding of device performances.
- In some cases, satisfying DOEs values are related to great dispersion in the values used to establish KCRV: that large dispersion (i.e. u(x_{ref})) compensates for discrepancies.

Regarding samples and reliability of the data, it is possible to say:

- The RM design ensured also high position and alignment repeatability.
- Peculiarities of black and glossy sample, put measuring device and laboratory measurement procedure under great stress and do not provide reliable and useful data, so the evaluation of the instrument performances with such kind of RM is useless, no KRCV is calculated for samples GK000 and GK210
- Laboratory R326 is an outlier in most of the measurement conditions and it is excluded from the calculations of KCRV
- Grey and diffuse samples provide better laboratory agreement among laboratories than the diffuse black samples
- To investigate if relevant discrepancies can be related to errors in data management or (if it is the case) algorithms and calculations
- Few single values are strong outliers, maybe because errors in the r-values calculations

4 LUMCORUN UNCERTAINTY SOFTWARE

The program applies to uncertainty computation of portable and laboratory instrument measuring luminance coefficient of road pavements studied in the project SURFACE [5]. The main aim is to provide an efficient computation of uncertainty contributions related to geometric errors or characteristics which require extensive calculation.

The program separately considers photometric errors and geometrics errors, the former depending mainly on non-geometric characteristics of the detectors and light sources (calibration, dark signal, linearity, temperature effect, stability, …) and the latter depending on geometric or spatial characteristics (detector aperture, goniometric (angles) errors, misalignments (sample)). The former can be calculated once, considering characteristics being constant at any measurement angles, and the latter must be calculated for each measurement angle to take into account the angle dependant effect of the BRDF on the error: aperture effect is negligible in a lambertian diffusing angular region but is critical around the specular angular peak.

The two uncertainty contributions can then be combined using uncertainty propagation rules as defined by the GUM

Given the diversity of instruments, the program could not cover all influent parameters for photometric errors and properly combine them; complementary calculations accounting for instrument's specificities should be designed and can be introduced as supplementary correction factors. Calculations tools are given for spectral mismatch and linearity error. For geometric errors most of the instrument cases are covered.

The general approach of the program is to use Monte Carlo Method (MCM), defined by the GUM supplement 1 But computation involving sampling of the sensitive detector area, light source emitting area and pavement sample area is not optimized for that case with random generation of spatial points, using predetermined regular spatial meshes enable to compute once all possible angles between point and then reuse them gaining processing time.

Notes:

It should be noticed that the aperture effect can lead to important systematic errors for angles around the specular direction, the GUM recommends to correct the systematic error and if it not possible to compute a pseudo-uncertainty from the dispersion around the mean of the systematic error over the range of parameters, here the incident angle ranges (see F.2.4.5 Uncertainty when correction from a calibration curve are not applied). The program does not apply this "replacement method" because the aperture errors is not significant in the non-specular region and could be very high in the specular region depending on the sample specularity and instrument characteristics, then an uniform uncertainty, i.e. applying for any angle, will overestimate and underestimate all the measurements.

But the user can use the program to performing a detailed calculation of aperture effect, export the data to a spreadsheet and apply her method to derive an uncertainty from dispersion of the systematic error with the measurand corrected from the mean of the systematic error.

If probability density function of the output quantity is available a coverage factor can be obtained. Due to the number of measurements of luminance coefficient, for a set of angles, and tedious calculations the PDF of geometric contribution for each angle is not registered. Then the PDF is not available, a practical coverage factor of 2 for a coverage interval corresponding to a coverage probability of 95% is recommended assuming that the distribution function of the measurand is Gaussian . It has been observed that the PDF of geometric contribution is in average Gaussian and that the PDF of photometric contribution, depending on several

random distributions, tends to be Gaussian, this last distribution can be visualised and checked with the program as well as the coverage probability for an coverage interval at ± 2 standard deviation for the mean.

4.1 Geometrical effects

The current version of the programme assumes:

- the detector spatial sensitivity is constant through its aperture, as well as the angular sensitivity (could be added)
- the illumination of the sample is uniform (non-uniformity could be added)

The geometrical effects are relevant for both absolute and relative measurements. For relative measurement data with used references (diffuse tile, Spectralon, ...) are missing, then we first assume a Lambertian behaviour. For absolute measurement or relative measurement geometrical effect must be sorted case by case with the measurement method and calibration method. For instance effects of non-overlapping of illuminated and viewed area while measuring a sample can be cancelled if the same non-overlapping occurs while measuring the reference, but the effective measured area size and position and size will impact the measurement for the sample.

4.1.1 Aperture effect (regular spatial mesh)

The aperture effect is computed to account of aperture or beam divergence resulting in angular integration of the BRDF.

For non-collimated beam the computation is based on a regular bi-dimensional mesh of involved areas (light source, detector, and sample), converted in 3D space by relevant rotation. The effective area, depending of the instrument, can be the illuminated area or the viewed area by the detector (programme selection). For each light source directions (Θi_n, ϕi_n) and for each sample point (m) incident ray angles from all illumination points (k), i.e. ($\Theta i_{n,m,k}$, $\phi i_{n,m,k}$), and reflected ray angles to all detector points (l) are computed, i.e. ($\Theta r_{n,m,l}$, $\phi r_{n,m,l}$). Once angles calculated the quantity $BRDF(\Theta i_{n,m,k}, \phi i_{n,m,k}, \Theta r_{n,m,l}, \phi r_{n,m,l})$ is summed over m, k, l indices with no weighting, the sum is divided by m x k x l to give the average value. Relative difference between integrated BRDF model and BRDF model is registered for all illumination directions (n), RMS and extrema values are given.

For collimated beam an identical implementation is used, but with the sample points limited to the sample centre point, and the illumination or detector area considered is bounded by the beam divergence.

The computation at a resolution of 0.2° for the testing example in section 6, is fast and lasts about 20 s, but at a resolution of 0.1° the number of operation is 4X4X4 times longer, which would lead to about 20 min of computation time.

4.1.2 Detector position (relative to α) (MCM)

Given that the luminance coefficient can vary significantly with the detector position, related to the uncertainty of α, a Monte-Carlo Simulation is used with a distribution of α. The BRDF function with angles from centre to centre (light source-sample, detector-sample) is used for that effect with no sampling. Implementing aperture sampling and random generation of detector position would provide a very long computation.

The available probability distributions are uniform, normal, and triangular.

- Uniform distribution should be used if there is no knowledge of the distribution of the input quantity

- Triangular distribution should be used is the input quantity has no chance to reach the upper and lower limits
- Normal distribution should be used if the input quantity is varying according to well know typical distribution (thermal noise, …)

4.1.3 Sample alignment in the horizontal plane (MCM)

This effect can be calculated with two fixed angles of the sample, which applies for devices having a rotating light source around the sample or a set of fixed light sources, or an equivalent design. It should be noticed that the misalignment of the sample, rotating in the zx plane change the relative detector position (α).

The BRDF function with angles from centre to centre (light source-sample, detector-sample) is used for that effect with no sampling.

The available probability distributions are uniform, normal, and triangular.

4.1.4 Illumination and detection area position and overlapping (regular spatial mesh)

This effect is possible if illuminated area or viewed areas are shifted from the reference centre. This effect is included in the "aperture effect" computation, taking into account the interface parameters: viewed and illuminated area size and position. The effective area of the sample illuminated and view by the detector is computed as the intersection of viewed and illuminated area.

Relative measurement selection means the reference measurement and sample measurement are done in the same conditions specified by the interface parameters: shifts from the centre are introduced as x, y offsets. Absolute measurement selection (via the IHM) means the reference measurement is done in the ideal position: i.e. overlapped and centred illumination viewed areas and the sample measurement with the interface parameters is done with the introduced shifts from (x, y offsets). Practically that changes the measurement of the sample by the ratio of the surface (shifted/ideal), the reference signal being a sum over the effective area of a constant BRDF.

Shifting the effective area in the horizontal plane without changing its size (still overlapped) has an impact on the measurement results, since that globally change illumination and viewing angle.

4.1.5 Illumination and detection alignment (relative to β) (MCM)

The uncertainty on angle β can have an impact on the measurand, especially around the specular direction, and depends on the detector position as well as illumination position, and then can be processed from uncertainty on β as the combination of deviation of position of the detector and illumination source.

4.2 Examples

Testing example: Aperture effect for circular aperture and non-collimated beams with an eccentric illumination inside the detection field

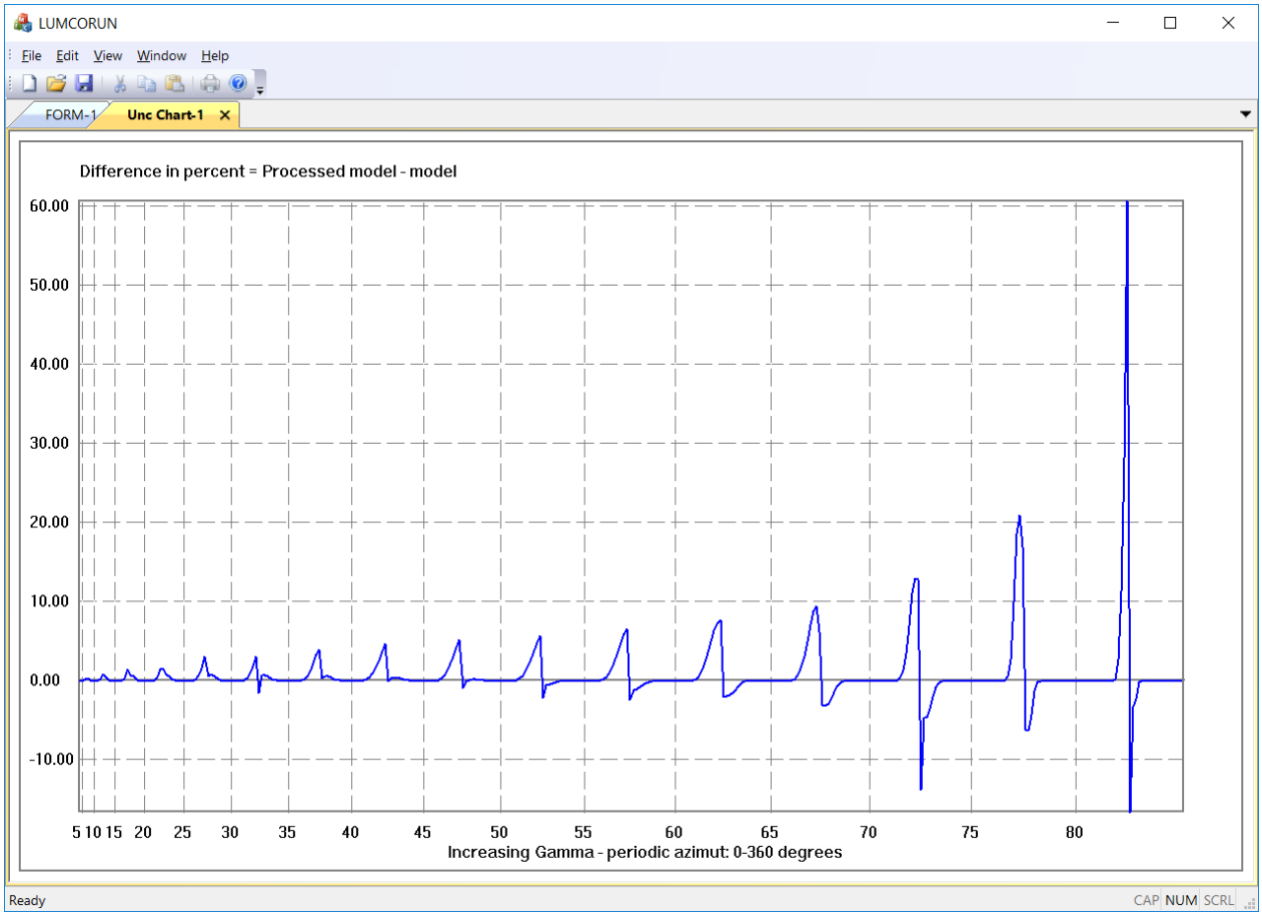

Figure 2: Aperture effect: Graph of relative differences % (model / integrated) using the CIE R3

Comment: this graph must be compared to the graph of 1.a, the conditions are the same with an eccentric illumination area (distance from centre along x, y axes: 5 mm). The detection and illumination are still overlapped (detection area in 1.a is changed to 70x70 mm²), the relative differences are higher with an asymmetric profile around the specular direction due to change of illuminating/viewing angles and high peak values.

Testing example: Effect of sample misalignment, uncertainty of 0.2° of the horizontal plane in two directions with uniform distribution

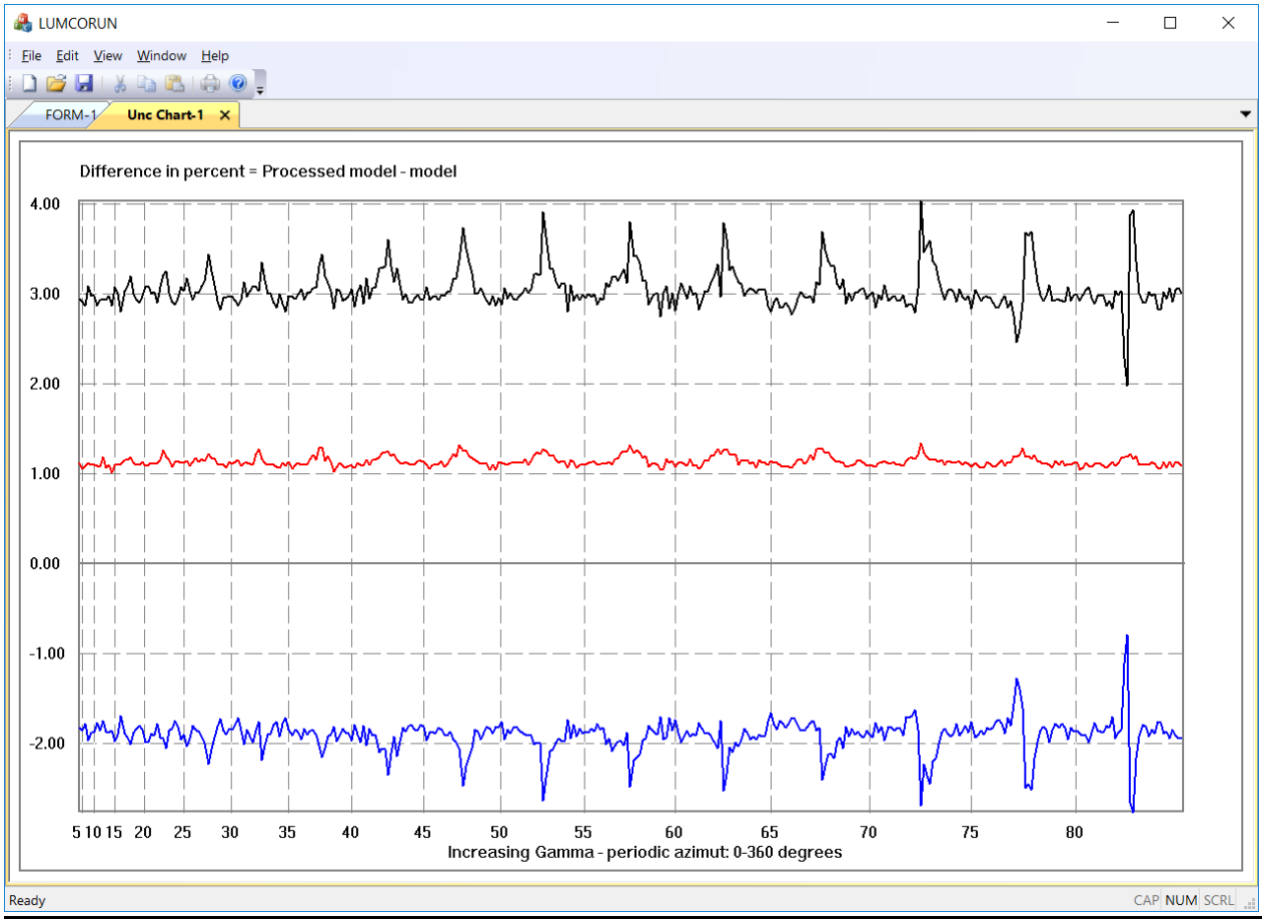

Figure 3 Uncertainty of sample alignment: 0.2° with uniform distribution (METAS sample)

Comment: Three curves are plotted. The blue one is the curve of the relative differences between the BRDF (simulated) and the mean of BRDF values obtained by MCM with the uniform distribution of angles. The red one is the curve of the relative the standard deviation of the BRDF values obtained by MCM with the uniform distribution of angles. The black one should be the resulting uncertainty, here temporarily calculated as the sum of the two others. The number of trials is 300 for each incident direction (Θi, ϕi), which yields to 90000 trials for each BRDF values (still noisy). The negative value of the mean curve (blue) is due to the asymmetric decrease of BRDF with the relative α between misaligned sample and detector.

Testing example: Effect of detector position, angle α = 1° with an uncertainty of 0.2° with uniform distribution

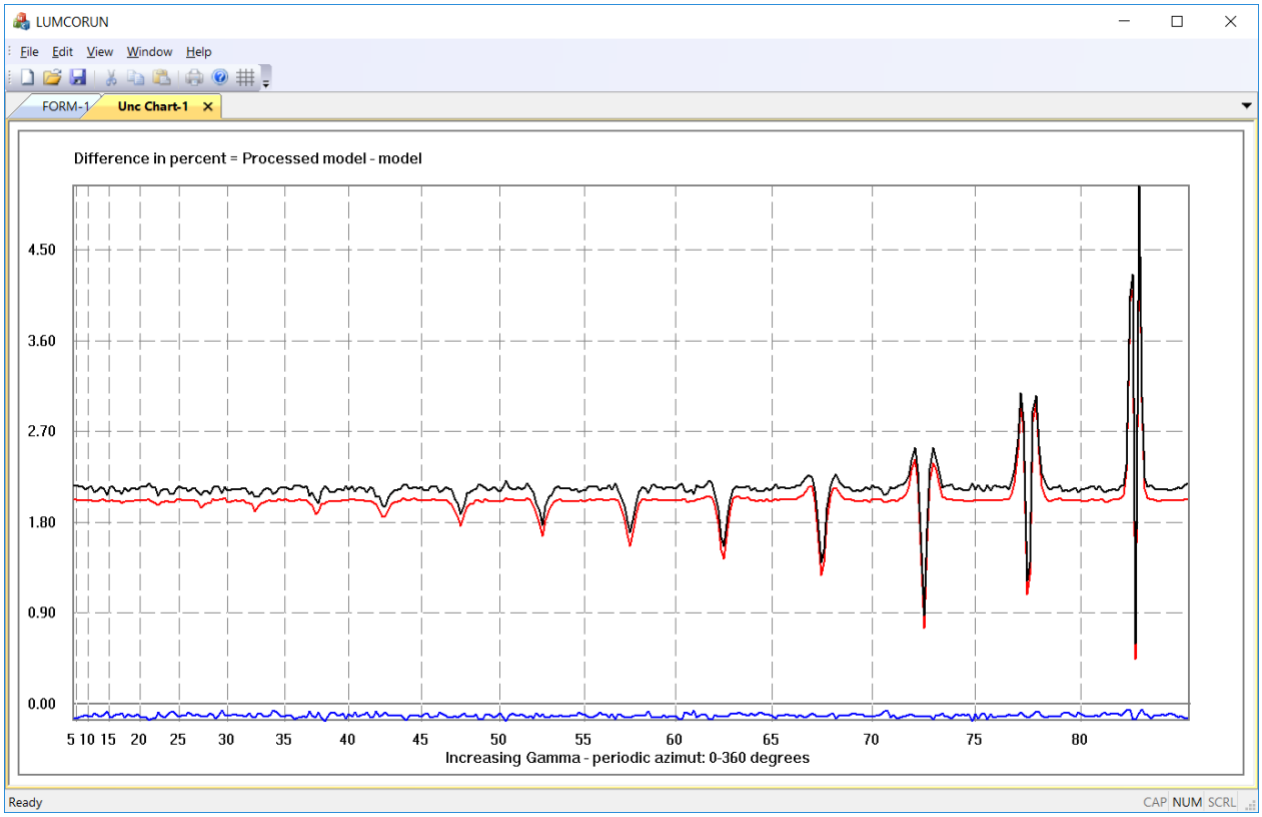

Figure 4 Uncertainty of detector position (α): 0.2° with uniform distribution (METAS sample)

Comment:

Three curves are plotted. The blue one is the curve of the relative differences between the BRDF (simulated) and the mean of BRDF values obtained by MCM with the uniform distribution of α. The red one is the curve of the relative the standard deviation of the BRDF values obtained by MCM with the uniform distribution of α. The black one should be the resulting uncertainty, here temporarily calculated as the sum of the two others. The number of trials is 10000. The negative small value of the mean curve (blue) is due to the asymmetric decrease of BRDF with α. This computation does not take into account the aperture effect.

5 CONCLUSION

Unfortunately, the Pandemic situation of COVID-19 had deep impact on the measurement intercomparison and data analysis including test on reliability of uncertainty software: laboratory access and staff involvement have been reduced and the current situation limits and/or hampers additional investigations especially on uncertainty evaluation and impact of the geometrical effects of source detector complex system.

The intercomparison show a poor agreement between participants, slightly better performances are achieved when considering integral values or higher tanε values, especially with grey samples.

Results indicate systematic issues and that the uncertainty evaluation requires further work: investigations should be focused on the impact of geometries of measurement and detector and lighting performances (acceptance and viewing area) and their mutual correlations and with the uncertainty. LUMCORUN software will be a useful tool for all participants.

6 APPENDIX A – PECULIARITIES OF MEASURING INSTRUMENT OF INTERCOMPARISON PARTICIPANTS

Excerpt from the descriptions provided by the participants.

6.1 CEREMA

The Cerema gonioreflectometer in Clermont-Ferrand measures the reflection of road surfaces under the observation conditions of a motorist at different observation angles:

- 1° according to CIE specifications,
- 2.29°, 5°, 10°, 20° and 45° by switching the metallic holders of the camera (see picture (c) of Figure 3)

It gives the 580 reflected luminance coefficients q(β, γ) of the r-table, and the parameters Q0 and S1. The mechanical positioning unit consists of a steel base on which is adapted a rotating measuring arm to change the sight angle β from 0 to 180° and a light source positioning system to vary the angle of incidence of light γ from 0 to 90° (Figure 5). The mechanical movement system of the lamp and the arm carrying the photometer is computer controlled, so the data acquisition is fully automated.

The reference source is a type A halogen lamp (Philips PAR38 Spot bulb with a power of 120W, a nominal voltage of 24 V, a nominal flow rate is 1545 lm) with a color temperature of 2700K (warm light) and an angle of diffusion of 10°. The light source is a fixed on a metal arc with a radius of 2.05 m, whose movement corresponding to the incidence angle is ensured by a motor connected to an indexer-transformer.

The illuminated area is a 10×10 cm square, always at the center of the sample. The “sample holder device” consists of a turntable allowing to adjust the height of the sample, its lateral positioning and inclination to obtain the horizontality of the sample upper surface (Figure 5b). This allows the measurement area to be centered on the sample without having to change the luminance meter and source settings.

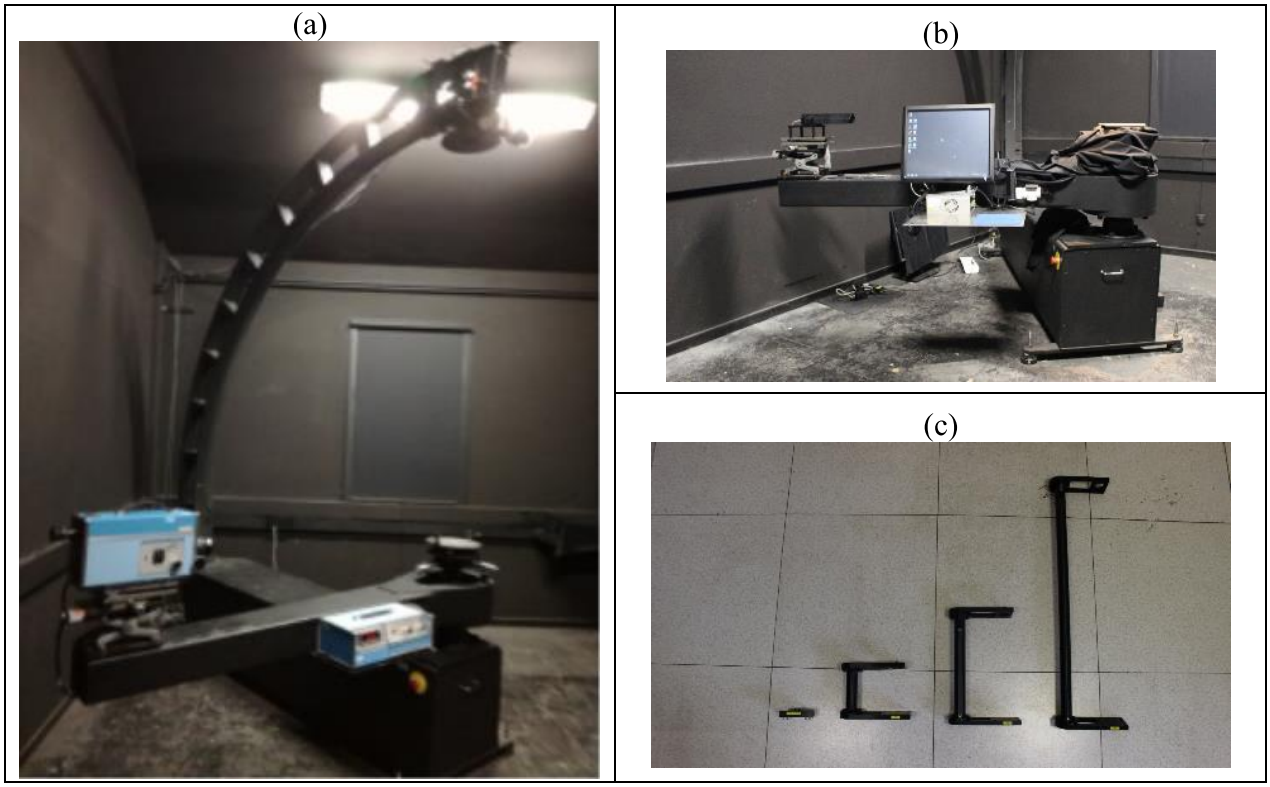

Figure 5 Pictures of the Cerema gonioreflectometer with the now replaced Pritchard photometer (a), the new camera with the computer operating it (b), the different metallic holders of the camera (c)

The luminance sensor was a Pritchard PR1980A Luminancemeter (see picture (a) of Figure 5) until 2019 September when it was replaced and upgraded with a camera Allied Visio Mako G419B (see picture (b) of Figure 5). This is a 12-bit monochrome CMOS camera with a global shutter. CMOS technology allows you to select a region of interest (ROI) on the sensor and capture only that area. In this situation, the ROI is the projection of the 10x10 cm square on the sample. The definition of a quite small specific ROI also allows high acquisition frequencies (typically 100 Hz) that are only limited by the exposure time. The resolution is 2048 x 2048 and the camera is equipped with a spectral luminous efficiency filter, V(λ) as defined by the CIE.

This camera is fixed on an articulated arm, made of light alloy that is driven by a gear motor for the 20 positions of β from 0 to 180°. The electronic control unit includes an indexer-translator which, in conjunction with the microcomputer, controls the stepper motors of the source carriage and the turntable.

A Labview program manages the control and data acquisition process and calculates the photometric parameters of the sample such as the luminance coefficient for all the angular combinations considered, the average luminance coefficient and the specular factors. The program ensures the presentation of the results in the form of a matrix of reduced luminance coefficients (r-table) and its corresponding reflection indicatrix.

6.2 METAS

Table 7 METAS Instruments characteristics

Name	LaFOR	MoFOR	LTL
Location	CH	CH	CH

Illumination	Source scan	source scan	8 sources
Source angul. subtense	0.5°	9.5°	1.1°
Detector angul. subtense	1.1°	0.7°	1.1°
Observation angle α	1°		
r-table	yes	yes	no
Q_0	yes	yes	Lin. combination
S_1	yes	yes	yes
Meas. field size	>100cm^2	78.5cm^2	56cm^2
Specificities	Absolute L, E	calibration	

6.3 IFSTTAR – UGE

A detailed presentation of the gonioreflectometer, its measurement and calibration procedures can be found in the paper presented at the CIE midterm meeting in 2017 at Jeju[25]

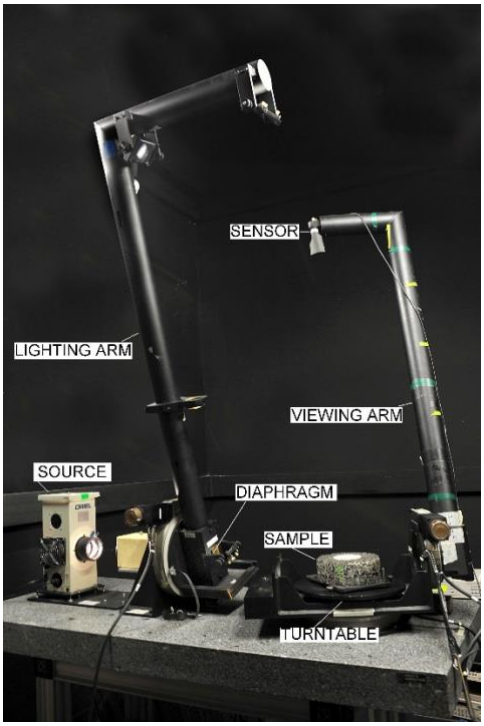

Figure 6 The gonioreflectometer of Univ. Gustave Eiffel

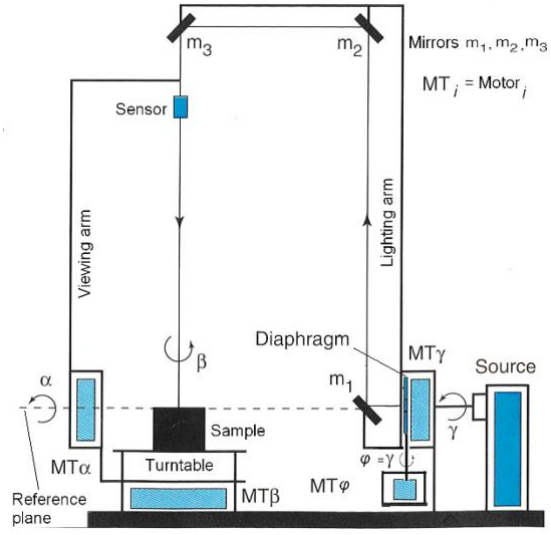

Figure 7 Diagram of the gonioreflectometer

Figure 6shows a picture of our gonioreflectometer. Figure 7presents its function diagram. The gonioreflectometer comprises a lighting unit harbouring a 250 W still halogen lamp powered by a stabilized power unit at a voltage of 23,8 V. The position of the lamp filament is adjusted so as to have it centred along the reference plane level. Additional optical elements (reflectors at its back and focusing lenses at its front) contribute to a collimated beam exiting the lighting unit. Next to this unit is a 150 cm long rotating lighting arm equipped with mirrors (m_1, m_2 and m_3) on its corners. Orientations of these mirrors are adjusted in order to steer the collimated beam coming out of the lighting unit, onto the sample. The lighted (and measured) area on the sample is a disk of 9,8 cm in diameter. The sample is laid on a rotating turntable which is fixed to a 150-cm long rotating viewing arm at the end of which is placed a photometer head. This sensor comprises a

photopic luminous efficiency function V (λ) filter and measures the illuminance reflected on it in a given direction from the lighted sample. The photometer head has a calibrated luminous responsitivity (ratio of an electric current and an illuminance) and its measurable output is an electric current. This current is amplified by a gain G and converted into a voltage thanks to an amplifier/converter. The converted voltage is read by a voltmeter and constitutes the measured value in fine for any set of angles (α, β,γ).

Our gonioreflectometer was designed for grazing lighting angles (up to 85° from the vertical, i.e. γ from 0° to 85°) and even more grazing viewing angles (down to 1° from the horizontal, i.e. $\alpha$from 1° to 90°). It also closely approaches retroreflection (as near as 2,5°). Besides these geometrical and optical constraints, independent motions of the lighting arm (whose motion defines γ), the viewing arm (viewing angle α), and the turntable (angle between the lighting and viewing planes β), ensure that the gonioreflectometer measures half a hemisphere above the sample, and by plane symmetry, the whole hemisphere.

Motions of the various components of the gonioreflectometer, via monitored motors, as well as measurements are all performed automatically thanks to in-house software developed with a visual programming environment.

The luminance coefficient q is generally determined by means of luminancemeters or ILMD (Imaging Luminance Measurement Devices). Instead, in our case, only illuminances on the photometer head are measured: after a prior calibration phase using the photometer head and a calibrated lambertian surface, we use the same sensor during the measurement phase, to indirectly determine both the luminance L and the illuminance E, and thus q.

The expression of q (=L/E), after taking into account the calibration phase, is as follows:

$$q(\alpha,\beta,\gamma)=\frac{\rho}{\pi\sqrt{2}\sin\alpha}\frac{E_r(\alpha,\beta,\gamma)}{E_d(\gamma)}$$

where

q is the luminance coefficient,

$\rho$is the reflectance of the spectralon obtained by calibration for a 0°/45° geometry;

$\alpha$is the viewing angle;

E_r is the illuminance reflected from the sample and measured by the sensor;

E_d is the illuminance reflected from spectralon whose BRDF is known by calibration, and measured by the sensor during a prior calibration phase.

6.4 NMF

The box has been developed by the NMF, which is a body for the improvement of road equipment that includes road administrations and institutes in the Nordic countries of Denmark, Finland, Iceland, Norway and Sweden. The box has already been used for quite extensive measurements on roads in Denmark, Finland and Sweden. The measurements are expected to continue on roads in Norway this year.

The box is described in the report "*A box for the measurement of road surface reflection properties*" version 21 February 2018 (can be downloaded from nmfv.dk). However, there is a simplified description of the box in section 1 on "*Instrument characteristics*" and section 2 on "*Stability of measurement and calibration*".

The main feature of the box is that it measures only two characteristic reflection values, called r_1 and r_2, but does this in accordance with basic requirements for sound measurements including limitation of aperture angles, stability and calibration. The two values represent respectively diffuse reflection and specular surface reflection – both as scattered in the surface texture of a road surface.

The two measures of total reflection, Q0 and Qd, are derived from r_1 and r_2 values by regressions based on a large number of r-tables. The specular factor S1 is defined by the ratio r_2/r_1.

6.4.1 Instrument characteristics

The principles of the NMF box are shown in figure 1.

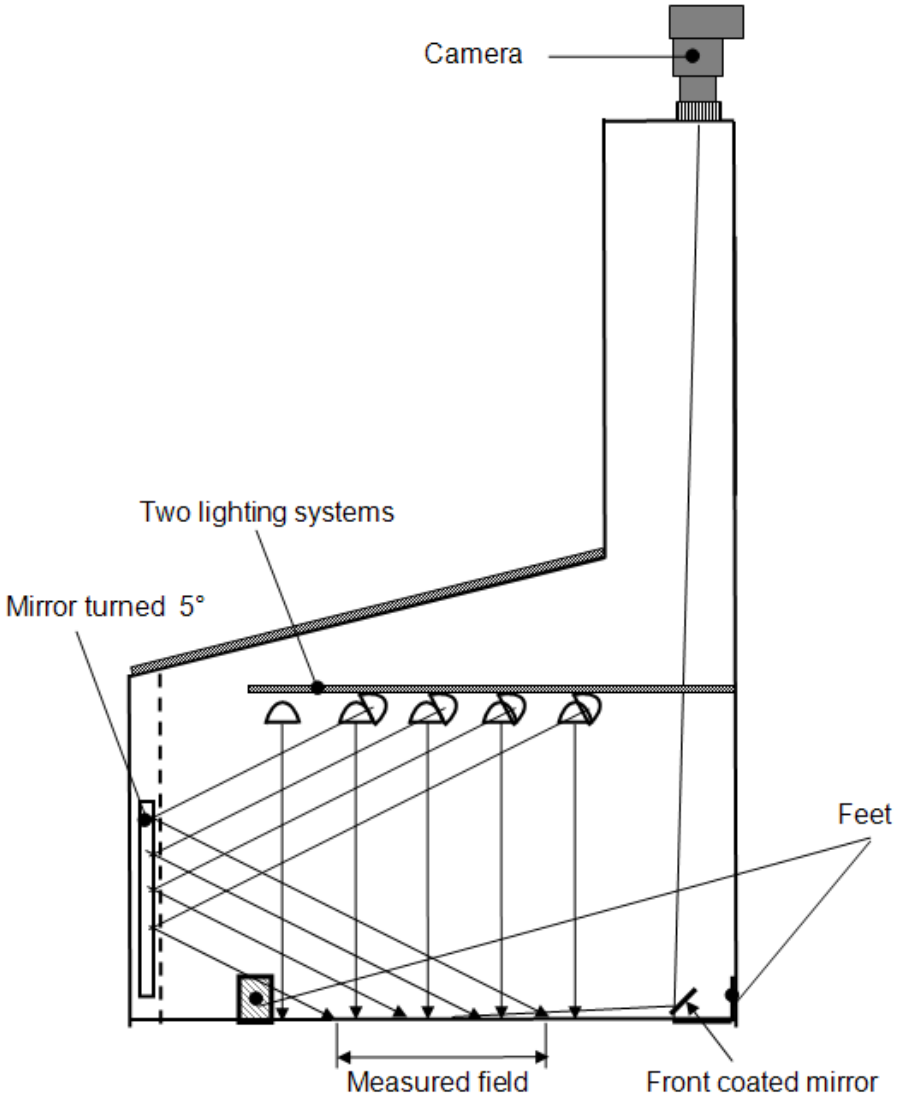

Figure 8 Principles of the NMF box.

The box has three feet on which it stands on a road surface to be measured. Two lighting systems provide illumination on the road surface and a camera is used to measure the luminance of a measured field.

The two lighting systems each include a number of lamps that provide quite uniform illumination over a measured field on the road surface. They are used in turn to measure two r-values, respectively r_1 and r_2 corresponding to entrance angles γ of respectively $\tan(\gamma)=0$ and $\tan(\gamma)=2$. The side angle β for r_2 is 0°. These are the r-values used to determine the specular factor S1 by $S1=r_2/r_1$.

The lamps for r_1 illuminate the measured field directly, while the lamps for r_2 illuminate the measured field through a mirror. This serves to reduce the length of the box.

The angular spread for r_1 is approximately ±5°, which is permissible for the measurement of r_1. The angular spread for r_2 needs, on the other hand, to be small in other to achieve a true result – in particular in the side angle. Accordingly, this angular spread has been reduced to approximately ±1° by limitation of the width of the measured field and other means.

The r_1 illumination system provides illumination of more that 10.000 lx, while the r_2 illumination system provides approximately 2.000 lx. These levels, together with a matt black interior of the box and various other features, eliminates the need to take daylight penetration into the box into account.

The camera is an LMK mobile advanced from TechnoTeam. For practical reasons, the camera is placed on top of the box and has a view to the measured field through a front coated mirror at the bottom of the box.

The longitudinal position of the camera determines the observation angle α. The options are 1,00°; 1,50° and 2,29°.

6.4.2 Stability of measurement and calibration

Following figure shows a close-up of a camera image.

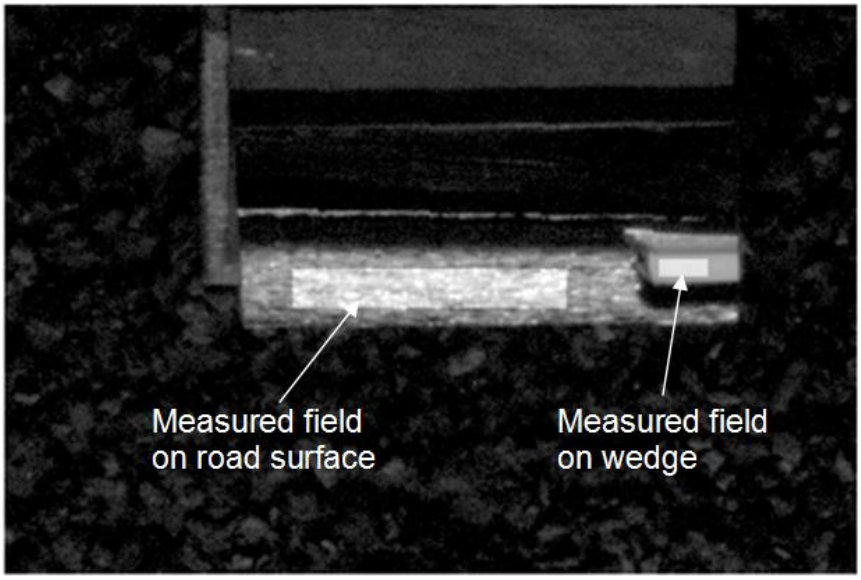

Figure 9: A close-up of a camera image.

Figure 9 shows that the box has an built-in wedge, which is illustrated in Figure 10.

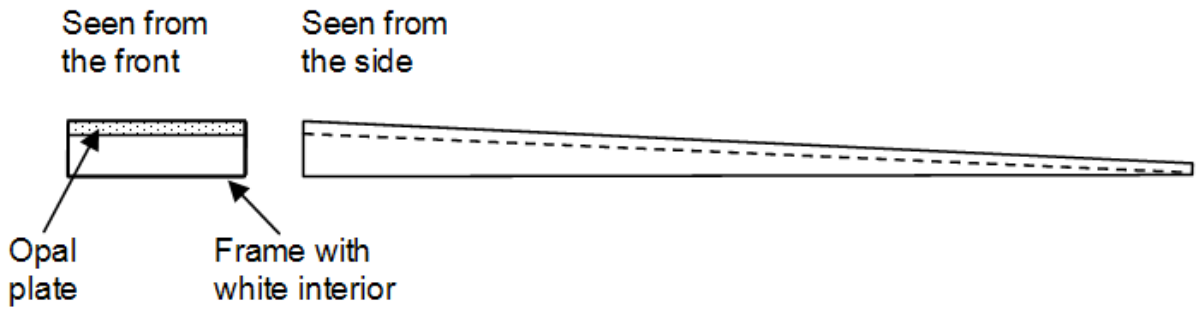

Figure 10: Built-in wedge.

Because of the construction of the wedge, the luminance in the opening is quite uniform and can represent the illuminance on the measured field. This way, gradual changes of the illuminance can be taken into account. The way to do that is to determine the r-value as the luminance of the measured field on the road surface in proportion to the luminance of the opening of the wedge – multiplied by a calibration factor.

The calibration factor is determined by measurement of similar wedge with a known luminance coefficient.

The luminance coefficient for r_1 illumination has been determined a number of times – the last time by RISE on 24 January 2020. The luminance coefficient for r_2 illumination is derived using the box and taking the levels of illumination for the two lighting systems into account.

7 APPENDIX B – REFERENCE MATERIALS AND MEASUREMENT PROCEDURE OF INTERCOMPARISON PARTICIPANTS

7.1 Reference materials

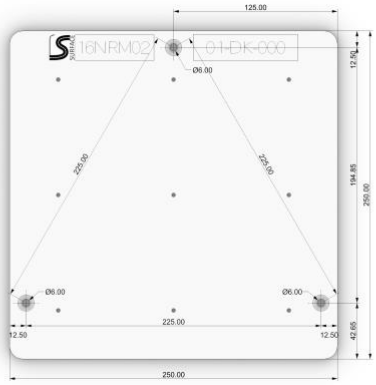

Figure 11 Frame of samples

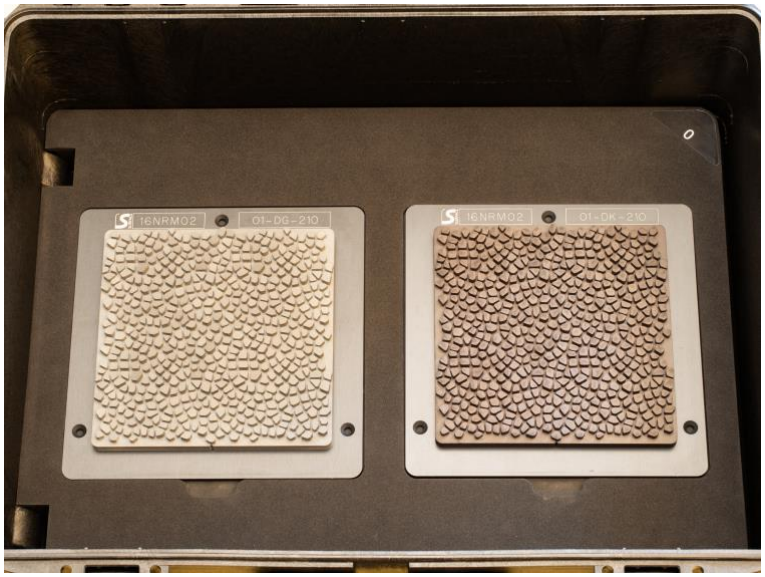

Figure 12 Samples DG210 and DK210

Figure 13 Samples DG000 and DK000

Figure 14 Samples GK210 and DG110

7.2 Intercomparison protocol measurement procedure

Excerpt from the intercomparison protocol:

The request is to measure the full r-table of all artefacts, or, since not all measuring devices are able to measure all tanε and β lighting angles as reported in Table 3 of EN 13201-3, at least for all measuring directions of the instrument and (if possible) for the directions at which the values will compared (Table 8) and for α=1° of observation.

If the measuring instrument is able to measure additional and/or non-conventional directions it is request to measure the samples also in the additional directions listed in Table 8 with

Table 9 observation angles.

The comparison of the values will be carried out for the directions listed in Table 8.

Table 8 Directions in which the measured values will be compared

Lighting Angles					Observation angle
tan ε	ε / °	β/ °		Additional β/ °	α/°
0	0	0	15	30	1
1	45				
2	63.43				
4	76				
6	80.5				
8	82.9				
11.5	85				

Table 9 Additional observation angles

Additional Observation angles α
2.29°
10°
20°

At least three measurements of each artefact and for each measuring geometry must be carried out, which means taking out the reference material before the next measurement.

The reduced luminance coefficient and Q0 and S_1 values of the artefacts must be measured following the measuring procedure of each laboratory for the given observation angles.

7.3 CEREMA

The measurement protocol is the following:

1. Positioning of the sample on the sample holder (see Picture (a) of theFigure 15). Orientation, height and inclination of the sample are then set in order to the camera to aim the correct area with the correct observation angle (see Picture (b) of theFigure 15).
2. Measurement of the source level of illumination at the level of the measurement area on the sample with an illuminancemeter. The value (Eh in the Equation (1)) is entered into the software for the calculation of the luminance coefficient. (see Picture (a) of the Figure 16).
3. Measurement of the luminance on a reference sample. A reference test is performed on a perfect diffuser (spectralon 99%, picture on Figure 16) to check the luminance values and shape of the measured diffusion indicator, thus attesting correct functioning of the goniophotometer. (see Figure 16(b)).
4. Then the test is carried out as follows: the lamp is in the first position (angle γ=0°), the arm rotates: the angle β varies and luminance measurements are taken for 20 β values over a half turn (between 2 and 180°). The γ angle varies for its 29 positions and measurements are still taken each time for the 20 values of β, for a total of 580 values.
5. Finally, the software calculates complete r-table, then computes Q0, S1 and S2

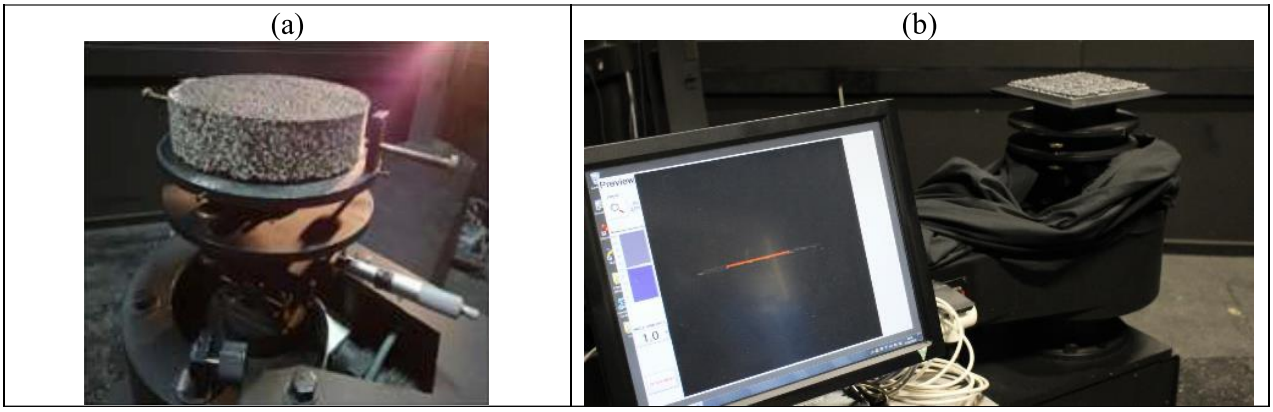

Figure 15 Picture of the sample holder device (a) and the sample positioning process thanks to the goniophotometer software

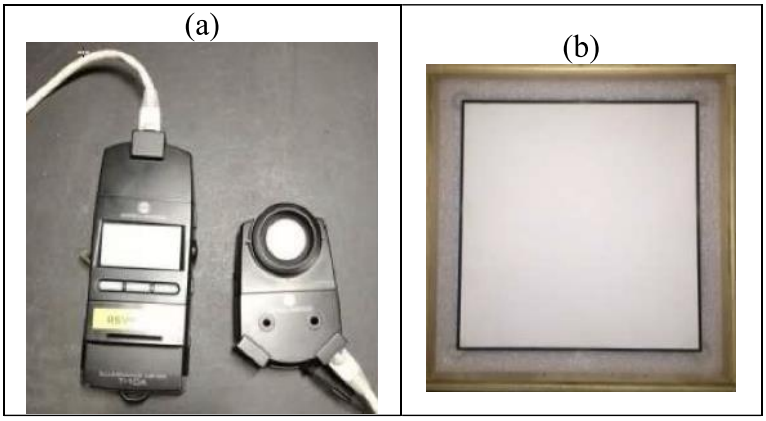

Figure 16 Picture of the illuminancemeter (a) and the perfect diffuser (spectralon 99%) (b)

7.3.1 Calibration procedure:

As described above, before each series of tests, in practical at the beginning of each test day, a reference test is performed on a perfect diffuser to check the luminance values and shape of the measured diffusion indicator, thus attesting correct functioning of the goniophotometer. There is also a measurement of the source level of illumination at the level of the measurement area on the sample with an illuminancemeter. Indirecltly, this also enables to attest the correct functioning of the light source.

7.3.2 Description of the measurement uncertainty model

No uncertainty model is used yet. We are waiting for the outputs of the Empir SURFACE project.

7.3.3 Additional information

All the measurements were done in a quite stable environment with less than 5° of temperature change. The humidity was not measured.

7.3.4 Presentation of the results

There is four files : 1°, 2.29°, 10° and 20°. For each measurement configuration and sample, there is a sheet with the data of the 3 measurements of the r-table are given with Q0 and S1.

On the second sheet, there is a table with the mean of the 3 measurements and the standard deviation computed with the classic excel formula

7.3.5 Remark on the measurements

It was not possible to get results measuring samples printed with the shiny dark material (01GK000 and 01GK210), except for 1° with the 01GK210 sample, but with poor standard-type values. It seems the Cerema goniophotometer software could not stabilize the luminance values because of the reflection and then it tried to do the measurement again indefinitely. With these very specular samples it seems that, within a single test, the luminance values goes from very low values to extreme high values, in a very unusual way compared to pavement samples.

To be noted, after the measurement campaign, this software was updated and measurement with these same shiny samples were possible to be made with the Cerema samples KIT. However, these results are of course not included in these inter-comparison campaign results.

There is a repetition missing with the 01DG110 sample for 1°, there is no explanation except that it seems the test has been forgotten. The two presented results are close.

There were 4 repetitions for the 01DG000 sample with 1°. This sample is visually not homogeneous and the third measurement was quite different from the two first. The fourth measurement is however close from the two first. It was then considered the third measurement has probably encountered a protocol anomaly (maybe sample placing) and the related results are not presented in the excel sheet.

7.4 METAS

The samples were measured three times each and for each instrument. The measurement of all the samples is referred to as a set. The measurements were done in laboratories with measured temperature within (22 ± 0.5) °C and humidity within (45 ± 5)%. The observation angle was always 1°.

LTL-200:

Two sets of measurement were made by one user, the last set by another user. The measurements were done over two days. Along the direction of observation, the illumination area was slightly larger than the size of the sample, which is a problem as the illumination would fall beside the surface, onto the sample holder. In the other dimension, the samples are bigger than the measurement area. Different parts of the sample were measured to try to keep the light on the sample**. But after checking the results, due to the size of the sample which were smaller than the illumination, it is not possible to use the results.**

MoFOR:

For this setup, the three set of measurements were each made on a different day, by the same user. The samples were always placed in the center of the illumination. The positioning is made by determining the center of the illumination field and centering the sample accordingly. The three sets of measurement were made one after the other so that the sample alignment was done for each measurement. The direction of measurement is determined with the help of the camera used for the luminance measurement and an alignment tool.

LaFOR:

Two sets of measurement were made by one person and the third one by another user. Each set of measurements took 2-3 days to make. To align the setup, the source is aligned to arrive perpendicularly on the sample, with the help of an adjustment laser. The sample is then aligned to the illumination field. The alignment of the samples along the direction of observation is subject to variations in the order of ±2mm, which slightly modify the measured zone.

7.4.1 Calibration procedure

The calibration procedure of the portable devices is made by measuring a reference plate and comparing adjusting to measurements of the same reference plate with the LaFOR setup. It is also used to compare the different setups and to make sure that the setups gives similar results over time. We currently do not have absolute reference values. The calibration is done once a year.

MoFOR:

MORFOR setup is used as a relative measurement devices. It has to be calibrated with some reference measurements made with LaFOR. To this effect, a reference plate consisting of a rather smooth surface is used (class R3). Different road extraction samples can also be use.

As the different samples exhibits very different properties, the choice of the reference material has an important impact. For the plates without structures, the reference plate measurement was used as a calibration as it also does not have structures. For the samples with structures, a road sample was used.

LaFOR:

The luminance and illuminance meters are calibrated once a year. As this is an absolute measurement, no other calibration is done. To verify the alignment and calibration of the setup, a reference plate is used to follow the evolution of the measurement through the years and make sure they stay consistent.

7.4.2 Measurement uncertainties

An uncertainty budget for each instrument is not yet available. Therefore, the uncertainties are computed as the standard deviation to the mean of the 3 measurements made for each sample. The following formula is used:

$$u(\bar{x}) = \sqrt{\frac{\sum_{i=1}^{n}(x_i - \bar{x})^2}{n(n-1)}}$$

This is done for the individual r-values and for the Q0 and S1 values. In excel this is done by using the following formula: STDEV.S(M1;M2;M3)/SQRT(3). Where M1, M2, M3 are the values from the three measurements.

7.5 IFSTTAR – UGE

We did all the measurements asked for, according to the instructions given in the document « INSTRUCTIONS FOR LUMINANCE COEFFICIENT INTERCOMPARISON KIT 1 ». In some cases, we could not, for lack of time, measure 3 times the same configuration. In some other cases, measurements were found to be aberrant (01-GK-000). So for these cases, there won't be any data provided in the respective field.

We have provided 4 excel files of data, respectively for 1°, 2.29°, 10° and 20° of observation angle.

7.5.1 UNCERTAINTY CALCULATIONS

Our instrument performance was evaluated, the conclusions[26] of which were presented during the 29th quadriennal session of the CIE at Washington D.C. (USA) DOI 10.25039/x46.2019.OP73.

One can refer to this paper for a detailed methodology to compute uncertainties, which includes A-type and B-type uncertainty calculations.

But due to lack of time, we coud not have the same number of reproducibility measurements for every sample and/or observation angle, and the maximum we could do is 3 measurements, which could not be enough for A-type calculations. We thus computed only B-type uncertainties, which in itself is quite sufficient to give an idea of the overall uncertainty. These uncertainties are provided in the excel sheets. If needed, one can easily compute A-type uncertainties from the available measurement data (by calculating a standard deviation).

7.6 NMF

The procedure for each artefact was:

a. an artefact was selected, and its height from bottom to the top surface was measured,

b. the box was lifted on its feet to the same height,

c. the artefact was placed inside the box with the right orientation and so that its longitudinal position is in the middle of the measuring field of the box,

d. photos for r_1 and r_2 values were taken with the camera at the location for an observation angle of 1,00°,

e. photos for r_1 and r_2 values were taken with the camera at the location for an observation angle of 2,29°.

The box was lifted by placing a sufficient number of thin aluminium bricks under each of the three feet.

In view of the relatively small width of the measuring field of the box, items d. and e. were carried out for three transverse positions of the artefact, so as to cover a width of its surface of 12 to 15 cm. All results are expressed as averages for those positions.

This procedure was carried out for each of the artefacts, and was repeated a total of three times.

The results were extracted from the photos by Kai Sørensen, whom also added derived values calculated by:

$Q0 = (0{,}957 \times r_1 + 0{,}746 \times r_2 + 104{,}5)/10.000$

$Qd = (0{,}981 \times r_1 + 0{,}323 \times r_2 + 86{,}1)/10.000$

$S1 = r_2/r_1$

The results are provided in tables 1 and 2 for the observation angles of respectively 1,00° and 2,29°.

Both tables present values for three repetitions of the measurements, labelled “first”, “second” and “third”. The averages and the standard deviations of the three values are also presented – for measured as well as for derived values.

8 APPENDIX C – PROVISIONAL DATA

Sample DK000

Discrepancies	A274				Discrepancies	R326				Discrepancies	Z927				Discrepancies	L864				Discrepancies	E289				Discrepancies	B492	
tg e	0,00	15,00	30,00		tg e	0,00	15,00	30,00		tg e	0,00	15,00	30,00		tg e	0,00	15,00	30,00		tg e	0,00	15,00	30,00		tg e	0,00	
0,00	1,19	1,22	0,77		0,00	1,04	2,27	2,22		0,00	1,33	1,39	1,63		0,00	0,07	0,04	0,72		0,00	1,42	1,67	2,17		0,00	10,51	
1,00	1,82	1,72	1,56		1,00	4,26	4,26	4,26		1,00	1,26	1,67	1,82		1,00	0,64	0,08	0,22		1,00	1,51	0,75	1,20		1,00	#DIV/0!	
2,00	0,85	1,61	1,62		2,00	7,16	7,44	7,40		2,00	1,95	1,71	1,80		2,00	0,96	0,02	0,19		2,00	1,61	0,24	0,85		2,00	6,60	
4,00	1,27	1,74	1,57		4,00	8,16	9,60	12,15		4,00	1,97	1,42	1,49		4,00	0,70	0,47	0,19		4,00	0,91	0,43	1,00		4,00	#DIV/0!	
6,00	1,47	1,69	1,73		6,00	7,27	8,49	15,95		6,00	1,91	1,50	0,96		6,00	0,43	0,36	0,67		6,00	0,88	0,82	0,92		6,00	#DIV/0!	
8,00	1,38	1,74			8,00	6,28	8,01			8,00	1,80	1,49			8,00	0,21	0,36			8,00	1,61	1,27			8,00	#DIV/0!	
11,50	1,49	1,96			11,50	6,95	10,06			11,50	1,19	1,10			11,50	0,10	0,85			11,50	3,49	1,37			11,50	#DIV/0!	

Sample DG000

Discrepancie	A274				Discrepancie	R326				Discrepancie	Z927				Discrepancie	L864				Discrepancie	E289				Discrepancie	B492	
tg e	0,00	15,00	30,00		tg e	0,00	15,00	30,00		tg e	0,00	15,00	30,00		tg e	0,00	15,00	30,00		tg e	0,00	15,00	30,00		tg e	0,00	
0,00	0,06	0,09	0,04		0,00	10,38	3,13	3,07		0,00	1,66	1,73	1,72		0,00	1,70	1,63	1,67		0,00	1,17	0,62	0,11		0,00	6,97	
1,00	0,96	1,42	1,38		1,00	4,22	3,88	4,44		1,00	1,97	1,76	1,59		1,00	0,92	0,17	0,08		1,00	0,32	0,20	0,00		1,00	#DIV/0!	
2,00	0,30	1,43	1,37		2,00	7,39	6,64	7,91		2,00	1,20	1,03	1,43		2,00	1,64	0,86	0,22		2,00	0,21	0,66	0,48		2,00	11,40	
4,00	1,65	1,22	0,51		4,00	10,05	10,55	14,70		4,00	1,79	1,43	1,29		4,00	0,13	0,30	0,75		4,00	0,03	1,30	1,42		4,00	#DIV/0!	
6,00	1,57	1,45	0,29		6,00	8,78	8,97	22,27		6,00	1,80	1,76	0,58		6,00	0,16	0,14	0,59		6,00	0,09	1,69	1,67		6,00	#DIV/0!	
8,00	1,62	1,36			8,00	8,34	9,58			8,00	1,82	1,89			8,00	0,19	0,45			8,00	0,92	2,53			8,00	#DIV/0!	
11,50	1,65	1,64			11,50	6,66	14,00			11,50	1,79	1,76			11,50	0,14	0,08			11,50	2,02	2,81			11,50	#DIV/0!	

Sample DK211

Discrepancie	A274				Discrepancie	R326				Discrepancie	Z927				Discrepancie	L864				Discrepancie	E289				Discrepancie	B492	
tg e	0,00	15,00	30,00		tg e	0,00	15,00	30,00		tg e	0,00	15,00	30,00		tg e	0,00	15,00	30,00		tg e	0,00	15,00	30,00		tg e	0,00	
0,00	1,99	1,93	1,83		0,00	0,45	0,40	0,27		0,00	0,96	0,98	1,11		0,00	1,02	0,98	0,77		0,00	0,13	1,16	1,51		0,00	2,21	
1,00	1,78	1,38	0,94		1,00	0,36	1,02	1,96		1,00	0,75	0,71	0,80		1,00	1,18	1,02	0,98		1,00	0,82	0,70	0,26		1,00	#DIV/0!	
2,00	1,93	1,83	0,63		2,00	1,40	3,17	4,31		2,00	0,66	0,57	0,54		2,00	1,21	1,30	1,32		2,00	1,90	0,19	0,29		2,00	4,81	
4,00	1,37	0,84	0,53		4,00	4,01	4,51	4,91		4,00	0,65	0,01	0,28		4,00	0,59	1,70	1,56		4,00	4,50	0,08	0,78		4,00	#DIV/0!	
6,00	1,42	0,42	0,38		6,00	8,18	5,44	3,87		6,00	0,88	0,23	0,31		6,00	0,48	1,82	1,85		6,00	5,75	0,10	0,96		6,00	#DIV/0!	
8,00	1,46	0,59			8,00	13,56	3,25			8,00	0,75	0,99			8,00	0,48	0,99	#DIV/0!		8,00	10,66	1,59			8,00	#DIV/0!	
11,50	0,98	0,26			11,50	10,49	1,93			11,50	0,73	0,99			11,50	1,46	1,99	#DIV/0!		11,50	13,28	0,66			11,50	#DIV/0!	

Sample DG110

Discrepancie	A274				Discrepancie	R326				Discrepancie	Z927				Discrepancie	L864				Discrepancie	E289				Discrepancie	B492	
tg e	0,00	15,00	30,00		tg e	0,00	15,00	30,00		tg e	0,00	15,00	30,00		tg e	0,00	15,00	30,00		tg e	0,00	15,00	30,00		tg e	0,00	
0,00	0,62	1,53	1,33		0,00	16,68	10,43	8,15		0,00	1,76	0,60	0,11		0,00	0,85	1,15	1,63		0,00	0,70	1,17	1,63		0,00	0,04	
1,00	0,54	1,57	1,46		1,00	12,13	10,82	9,37		1,00	1,45	0,26	0,29		1,00	0,12	1,27	1,85		1,00	0,84	0,65	0,30		1,00	#DIV/0!	
2,00	1,70	1,40	1,44		2,00	8,67	6,90	9,45		2,00	1,51	0,01	0,31		2,00	0,15	1,36	1,86		2,00	0,87	0,23	1,01		2,00	2,41	
4,00	0,06	0,97	1,46		4,00	13,40	8,11	9,47		4,00	1,38	0,94	0,12		4,00	0,95	1,88	1,63		4,00	3,61	0,38	2,39		4,00	#DIV/0!	
6,00	0,20	0,89	1,46		6,00	12,32	7,12	7,14		6,00	1,63	0,81	0,13		6,00	1,01	1,66	1,64		6,00	4,95	0,34	2,52		6,00	#DIV/0!	
8,00	0,52	1,33			8,00	11,14	4,88			8,00	1,64	0,40			8,00	0,81	1,84			8,00	9,76	1,67			8,00	#DIV/0!	
11,50	0,73	0,08			11,50	16,64	25,94			11,50	0,04	1,27			11,50	0,42	1,49			11,50	13,36	0,09			11,50	#DIV/0!	

Sample DG210

Discrepancie	A274				Discrepancie	R326				Discrepancie	Z927				Discrepancie	L864				Discrepancie	E289				Discrepancie	B492	
tg e	0,00	15,00	30,00		tg e	0,00	15,00	30,00		tg e	0,00	15,00	30,00		tg e	0,00	15,00	30,00		tg e	0,00	15,00	30,00		tg e	0,00	
0,00	0,34	0,35	0,28		0,00	0,01	0,24	0,18		0,00	0,23	0,20	0,23		0,00	0,11	0,14	0,04		0,00	1,25	1,29	1,38		0,00	1,50	
1,00	1,00	0,96	0,54		1,00	0,60	1,12	1,43		1,00	0,38	0,37	0,17		1,00	0,61	0,58	0,36		1,00	0,70	0,32	0,42		1,00	#DIV/0!	
2,00	0,74	1,00	0,57		2,00	1,69	2,40	2,79		2,00	0,21	0,19	0,05		2,00	0,52	0,80	0,52		2,00	0,71	0,10	0,09		2,00	1,45	
4,00	0,43	0,79	0,65		4,00	2,72	3,20	3,52		4,00	0,21	0,04	0,02		4,00	0,21	0,76	0,63		4,00	1,41	0,09	0,21		4,00	#DIV/0!	
6,00	0,42	0,80	0,53		6,00	3,18	3,47	3,87		6,00	0,31	0,32	0,24		6,00	0,10	0,50	0,29		6,00	2,33	0,47	0,65		6,00	#DIV/0!	
8,00	0,48	1,16			8,00	3,59	3,33			8,00	0,31	0,43			8,00	0,17	0,73	#DIV/0!		8,00	6,21	1,28			8,00	#DIV/0!	
11,50	0,53	1,06			11,50	3,62	3,59			11,50	0,06	0,32			11,50	0,56	0,73	#DIV/0!		11,50	10,97	1,00			11,50	#DIV/0!	

Sample DK000

Discrepancies	F331				Discrepancies	M844				Discrepancies	S351				Discrepancies	P811				Discrepancies	T031				Discrepancies	W112
Q0 value	2,55				Q0 value	3,98				Q0 value	0,78				Q0 value	0,18				Q0 value	3,28				Q0 value	1,80
S1 value	0,09				S1 value	1,11				S1 value	0,08				S1 value	0,11				S1 value	0,02				S1 value	0,11

Sample DG000

Discrepancie	F331				Discrepancie	M844				Discrepancie	S351				Discrepancie	P811				Discrepancie	T031				Discrepancie	W112
Q0 value	2,29				Q0 value	4,30				Q0 value	0,41				Q0 value	0,30				Q0 value	2,35				Q0 value	2,22
S1 value	0,01				S1 value	1,18				S1 value	0,08				S1 value	0,05				S1 value	0,17				S1 value	0,04

Sample DK210

Discrepancie	F331				Discrepancie	M844				Discrepancie	S351				Discrepancie	P811				Discrepancie	T031				Discrepancie	W112
Q0 value	1,86				Q0 value	2,35				Q0 value	1,50				Q0 value	1,76				Q0 value	2,85				Q0 value	1,38
S1 value	0,15				S1 value	0,46				S1 value	0,11				S1 value	0,12				S1 value	0,36				S1 value	0,16

Sample DG110

Discrepancie	F331				Discrepancie	M844				Discrepancie	S351				Discrepancie	P811				Discrepancie	T031				Discrepancie	W112
Q0 value	2,79				Q0 value	13,76				Q0 value	0,98				Q0 value	0,47				Q0 value	4,09				Q0 value	1,08
S1 value	0,05				S1 value	0,78				S1 value	0,27				S1 value	0,08				S1 value	0,06				S1 value	0,30

Sample DG210

Discrepancie	F331				Discrepancie	M844				Discrepancie	S351				Discrepancie	P811				Discrepancie	T031				Discrepancie	W112
Q0 value	0,88				Q0 value	2,19				Q0 value	0,54				Q0 value	0,34				Q0 value	1,96				Q0 value	0,00
S1 value	0,18				S1 value	0,77				S1 value	0,02				S1 value	0,28				S1 value	0,17				S1 value	0,08

9 REFERENCES

1. Road Statistics. Yearbook 2017 Road Statistics; European Union Road Federation: Brussels, Belgium, 2017., http://www.erf.be/wp-content/uploads/2018/01/Road_statistics_2017.pdf (accessed 28 March 2019).

2. Sorensen K, Nielsen B. ROAD SURFACES IN TRAFFIC LIGHTING, https://trid.trb.org/view/37817 (1974, accessed 24 December 2020).

3. EN 13201-3:2015. Road lighting - Part 3: Calculation of performance.

4. *CIE 144-2001 Road surface and road marking reflection characteristics*. Technical Report, CIE, 2001.

5. CIE 030:1976 Calculation and Measurement of Luminance and Illuminance in Road Lighting, http://cie.co.at/publications/calculation-and-measurement-luminance-and-illuminance-road-lighting (1976, accessed 16 March 2020).

6. CIE 030.2:1982 Calculation and Measurement of Luminance and Illuminance in Road Lighting, http://cie.co.at/publications/calculation-and-measurement-luminance-and-illuminance-road-lighting (1982, accessed 16 March 2020).

7. *CIE 066:1984 Road surfaces and lighting (joint technical report CIE/PIARC)*. CIE, http://cie.co.at/publications/road-surfaces-and-lighting-joint-technical-report-ciepiarc (1984, accessed 12 March 2020).

8. CIE 140:2000 Road Lighting Calculations, https://www.techstreet.com/cie/standards/cie-140-2000?product_id=1210058 (2000, accessed 18 March 2020).

9. Gašparovský D, Janiga P, Korobko A, et al. *CIE 140:2019 Road Lighting Calculations, 2nd Edition*. CIE 140:2019, International Commission on Illumination (CIE). Epub ahead of print 5 February 2019. DOI: 10.25039/TR.140.2019.

10. spectral luminous efficiency (of a monochromatic radiation of wavelength λ) [V(λ) for photopic vision; V'(λ) for scotopic vision] | eilv. *CIE e-International Lighting Vocabulary*, http://eilv.cie.co.at/term/1222 (accessed 18 March 2020).

11. Muzet V, Bernasconi J, Iacomussi P, et al. Review of road surface photometry methods and devices – Proposal for new measurement geometries. *LRT* 2020; 1–16.

12. Sørensen K. Q0 and Qd – "lightness" of road surfaces in road lighting.

13. Fan S, Liu M, Shen H. Uncertainty analysis of a pavement reflectance measurement system based on a gonio-photometer. *Chin Opt Lett* 2014; 12: 051201–051204.

14. Saint-Jacques E, Prevost C, Villa C. Evaluation of the performance of a road surface gonioreflectometer. In: *PROCEEDINGS OF the 29th Quadrennial Session of the CIE*. Washington DC, USA: International Commission on Illumination, CIE, pp. 536–545.

15. Muzet V, Paumier J-L, Guillard Y. COLUROUTE : a mobile gonio-reflectometer to characterize the road surface photometry. TURIN, ITALY: CIE, https://www.researchgate.net/publication/279258920_COLUROUTE_a_mobile_gonio-reflectometer_to_characterize_the_road_surface_photometry (2008, accessed 12 March 2020).

16. Maghe L. Characterization of Road Surfaces using a Mobile Gonio-reflectometer. TURIN, ITALY: CIE, http://cie.co.at/publications/proceedings-2nd-cie-expert-symposium-advances-photometry-abd-colorimetry-7-8-july-2008.

17. Casol M, Fiorentin P, Scroccaro A. On road measurements of the luminance coefficient of paving. Florence, Italy, https://www.researchgate.net/publication/237681358_On_road_measurements_of_the_luminance_coefficient_of_paving (2008, accessed 12 March 2020).

18. Corell D, Sørensen K. An instrument for the measurement of road surface reflection properties. In: *PROCEEDINGS OF THE CONFERENCE AT THE CIE MIDTERM MEETING 2017 23 – 25 OCTOBER 2017, JEJU, REPUBLIC OF KOREA*. Jeju Island, Republic of Korea: International Commission on Illumination, CIE, pp. 443–452.

19. Blattner P, Dudli H. Mobiles Fahrbahnoberflächenreflektometer. Bern: Schweizerische Lichttechnische Gesellschaft; Deutsche Lichttechnische Gesellschaft; Lichttechnische Gesellschaft Österreichs; Nederlandse Stichting voor Verlichtingskunde, 2006, p. 106 ff.

20. CIE Expert Symposium A New Vision of Visibility in Roadway Lighting, 25–26 May 2018, Berlin, Germany., https://surface-nrm02.eu/publications-presentations/ (accessed 28 March 2019).

21. Muzet V, Greffier F, Nicolaï A, et al. Evaluation of the performance of an optimized road surface/lighting combination: *Lighting Research & Technology* 2018; 51: 576–591.

22. Muzet V, Abdo J. On Site Photometric Characterisation of Cement Concrete Pavements with COLUROUTE Device. *Light and Engineering* 2018; 26: 88–94.

23. Muzet V, Greffier F, Verny P. Optimization of road surface reflections properties and lighting: learning of a three-year experiment. In: *Proceedings of the 29th CIE SESSION*. Washington D.C. (USA): CIE, 2019. Epub ahead of print 2019. DOI: 10.25039/x46.2019.OP72.

24. Pommé S, Institute for Reference Materials and Measurements. *Determination of a reference value, associated standard uncertainty and degrees of equivalence for CCRI(II) key comparison data.* Luxembourg: Publications Office, 2012.

25. Saint-Jacques E, Dumont E, Villa C. Characterisation of the reflection properties of road surfaces using an in-lab gonioreflectometer. Jeju, Korea: CIE. Epub ahead of print 12 March 2020. DOI: 10.25039/x044.2017.

26. Saint-Jacques E, Prevost C, Villa C. Evaluation of the performance of a road surface gonioreflectometer. In: *PROCEEDINGS OF the 29th Quadrennial Session of the CIE*. Washington DC, USA: International Commission on Illumination, CIE, pp. 536–545.